

# MHD CONVECTIVE HEAT AND MASS TRANSFER THROUGH AN AXIALLY VARYING PIPE WITH SORET EFFECT

B. Ramakrishna Reddy

Department of Mathematics, Gokaraju Rangaraju Institute of Engineering and Technology, Hyderabad, India

## Abstract

*We analyse the combined heat and mass transfer of an electrically conducting viscous fluid in a corrugated pipe in the presence of a constant heat source. A non-uniform temperature is maintained on the boundary. Taking the slope  $\delta$  of the boundary of the pipe as a perturbation parameter, the equations governing the flow, heat, mass transfer and magnetic induction have been solved. The velocity, temperature, and concentration have been evaluated for variations in the different governing parameters. The effect of the various governing parameters on flow, heat and mass transfer has been exhibited through various profiles of velocity, temperature and concentration distributions.*

## Keywords

*MHD, Axial variation, Soret effect, non uniform temperature*

## 1. Introduction

There are many transport processes in the Industrial equipment and in the environment in which buoyancy force arises from both thermal and mass diffusion as a result of the co-existence of the temperature gradients and concentration differences of dissimilar chemical species. In such a class of flows, the driving force is provided by a combination of thermal and chemical species diffusion effects. In atmospheric flows thermal convection resulting from heating of the earth by sunlight is affected by difference in water vapour concentration. This buoyancy driven convection due to coupled heat and mass transfer in porous medium has many important applications in energy related engineering problems.

In most of the studies pertaining to convection flows through the pipes, the axial dependence of the flow variables (2,4,5,6,9,10,12) is neglected and either the temperature or its gradient is maintained uniform on the boundary. Also the heat transfer analysis is investigated in the absence of any internal heat sources in the flow field. The heat transfer in a flow through a pipe in the presence of additional internal heat source has direct application to the modified chemical vapour deposition process. This MCVD process is being used to make high quality optical glass fibers (13,17,18).

Thermal convection problem in porous media occurs in a broad spectrum of the disciplines ranging from chemical Engineering to Geophysics. Applications include heat insulations by fibrous materials, spreading of pollutants, convection of Earth's mantle. A large cross-section of fundamental research has been carried out by several authors in the recent times. In most of the investigations the boundaries are uniform in cross-section as well as the boundary temperatures. However, there are a few physical situations which warrant the assumption of non-uniformity in either the boundaries or the boundary temperatures. In a convection flow through a channel such a non-uniformity creates a secondary flow. This secondary flow is of vital importance to technological process for example, the process of modified chemical vapour deposition MCVD (8,13) has been suggested in drawing optical glass fibers of extremely low loss and wide bond width.

In hydro magnetic case flow through channel with non-uniform gap has been considered by Mc Michael and Deutsch (11) in their paper on MHD laminar flow in the slowly varying tube in the presence of an axial magnetic field. They considered a small parameter  $\delta \ll 1$  (given by the ratio of radial to axial length scaling) which characterises the wall slope of the regions of varying radius. The problem is analysed as a regular perturbation problem at finite magnetic Reynolds number and Hartman number as large as  $O(\delta^{-1/2})$ . It is observed that the onset of flow separation is associated with adverse axial gradients of wall pressure created by radial magnetic body forces. These are produced by electric currents induced at first order by zeroth order stream lines crossing the uniform field, developing obviously large radial pressure gradients. The dimensionless current density is independent of the Hartmann and Reynolds numbers, so that the physical current density varies linearly with flow rate and applied field strength high current densities are localized in the vicinity of maximum wall slope near the half radius point. Magnetic effects, treated as first order perturbation to the basic local Hagen-poiseuille flow, lead to separation in both converging and diverging sections of the tube, while inertial effects promote separation only in diverging sections. The induced magnetic field affects the flow even at the first order as long as long

as  $(\delta, R_m)$  remains sufficiently small and thus the interactions between the induced field and the base flow are only of second order. This analysis has been extended by Deschikachar et al (3) to include the effect of unsteadiness on the flow. Such purely oscillatory flow over non-uniform surfaces that are not straight exhibits a steady stream caused by the non-linear equations governing the motion. This phenomena of steady streaming is of great mathematical and physical interest. The pressure and shear stress on the wall for various parameters governing the flow are discussed.

Krishna et al(8) have analysed the combined free and forced convection flow through an axially varying vertical pipe in the presence of an internal heat source of constant strength. Murthy(12) has extended this to study the effects of a uniform axial magnetic field. Costa(1) has analysed the viscous dissipation effects in natural and mixed convection heat transfer. Recently Basack et al(16) have discussed the natural convection flow in a square cavity filled with a porous heated bottom wall and adiabatic top wall maintaining constant temperature of cold vertical walls.

## 2. Formulation of the problem

We consider the steady axisymmetric flow of an incompressible, viscous electrically conducting fluid in a vertical pipe of variable cross section maintained at non-uniform temperature  $\gamma(\delta x/a)$ . The Boussinesq approximation is used so that the density variations will be retained only in the buoyancy force. The viscous dissipation is neglected in comparison to the heat flow by convection. The concentration on these walls is taken to be constant. The cylindrical polar system  $(r, x)$  is chosen with  $x$ -axis along the axis of the pipe. The boundary of the pipe is assumed to be

$$r = af(\delta x/a)$$

where 'a' is characteristic radial length,  $f$  is twice differentiable and ' $\delta$ ' is a small parameter proportional to the boundary slope. The flow is maintained by a constant flow for which a characteristic velocity  $U$  is defined as

$$U = \left(\frac{2}{a^2}\right) \int_0^{af(\delta x/a)} ur dr \quad (2.1)$$

The applied magnetic field  $B_0$  is uniform and directed along the axis of the pipe. No electric field is applied and there is no induced electric field for the constraints given(24). The electrical conductivity of the pipe walls remains arbitrary and without influence on the flow are

$$\rho_e (\zeta \bar{x} \bar{q}) = -\nabla p + \mu \nabla^2 \bar{q} - \left(\frac{\mu}{k}\right) \bar{q} + \mu_e (\bar{J} \times \bar{B}) - \rho \bar{g} \quad (2.2)$$

$$\nabla \cdot \bar{q} = 0 \quad (2.3)$$

$$\rho_e C_p (\bar{q} \cdot \nabla) T = \lambda \nabla^2 T + Q \quad (2.4)$$

$$(\bar{q} \cdot \nabla) C = D_1 \nabla^2 C + k_{11} \nabla^2 T \quad (2.5)$$

$$\rho - \rho_e = -\beta(T - T_e) - \beta^*(C - C_e) \quad (2.6)$$

The Maxwell's equations related to the magnetic induction vector  $\bar{B}$  are

$$\nabla \cdot \bar{B} = 0 \quad (2.7)$$

$$\nabla \times \bar{B} = 4\pi \bar{J} \quad (2.8)$$

The Ohm's law gives

$$\bar{J} = \sigma \mu_e (\bar{q} \times \bar{B}) \quad (2.9)$$

Where  $\rho_e$  is the density of the fluid in the equilibrium state,  $\bar{q}$  is the velocity,  $\zeta$  is the viscosity,  $p$  is the pressure.  $T$ ,  $C$  are the temperature and concentration in the flow region,  $\rho$  is the density of the fluid,  $k$  is the coefficient of permeability,  $Q$  is the strength of the heat source,  $\mu$  is the coefficient of viscosity,  $C_p$  is the specific heat at constant pressure,  $\lambda$  is the coefficient of thermal conductivity,  $\beta_1$  is the coefficient of volume expansion,  $\bar{B}$  is the magnetic induction vector,  $\bar{J}$  is the current density vector,  $\sigma$  is the electrical conductivity of the fluid,  $D$  is the molecular diffusivity,  $k_{11}$  is the cross diffusivity,  $\beta^*$  is the coefficient of expansion with mass fraction and  $\mu_e$  is the magnetic permeability.

In the equilibrium state

$$-\frac{\partial p_e}{\partial x} - \rho_e g = 0 \quad (2.10)$$

Where  $p = p_e + p_D$ ;  $p_D$  is the hydrodynamic pressure.

Introducing the non-dimensional variables

$$\bar{q}^* = q/U, p^* = p/\rho U^2, \bar{B}^* = B/B_0, \bar{J}^* = J/\sigma U B_0$$

$$\theta = \frac{T - T_e}{\Delta T_e}, C^* = \frac{C - C_e}{\Delta C_e}, \gamma^* = \gamma/\Delta T$$

$$\Delta T_e = T_e(0) - T_e(a)$$

$$\Delta C_e = C_e(0) - C_e(a)$$

The equations (2.2)-(2.9) reduce to (on dropping the asterisks)

$$R_e(\bar{\zeta}x\bar{q}) + \nabla(p + \frac{1}{2q^2}) + \nabla^2 q + M^2(\bar{J}x\bar{B}) - G(\theta + NC) \quad (2.11)$$

$$\nabla \cdot \bar{q} = 0 \quad (2.12)$$

$$P_e(\bar{q} \cdot \nabla)\theta = \frac{\partial^2 \theta}{\partial r^2} + \frac{1}{r} \frac{\partial \theta}{\partial r} + \frac{\partial^2 \theta}{\partial x^2} + 1 \quad (2.13)$$

$$R_e Sc(\bar{q} \cdot \nabla)C = \frac{\partial^2 C}{\partial r^2} + \frac{1}{r} \frac{\partial C}{\partial r} + \frac{\partial^2 C}{\partial x^2} + \frac{So}{N} \left( \frac{\partial^2 \theta}{\partial r^2} + \frac{1}{r} \frac{\partial \theta}{\partial r} + \frac{\partial^2 \theta}{\partial x^2} \right) \quad (2.14)$$

$$\nabla \cdot \bar{B} = 0 \quad (2.15)$$

$$\nabla x \bar{B} = R_m \bar{J} \quad (2.16)$$

$$\bar{J} = (\bar{q} x \bar{B}) \quad (2.17)$$

Where

$$R_e = \frac{Ua}{\nu} \quad (\text{the Reynolds number})$$

$$R_m = \sigma \mu_e u_c a \quad (\text{the magnetic Reynolds number})$$

$$M = aB_0 \left( \frac{\sigma}{\rho \nu} \right)^{1/2} \quad (\text{the Hartmann number}) \quad G = \frac{\beta_1 g \Delta T_e a^3}{\nu^2} \quad (\text{the Grashof number})$$

$$P_e = \frac{\mu_e U C_p a}{\lambda \nu} \quad (\text{the Peclet number}) \quad D^{-1} = \frac{a^2}{k} \quad (\text{the Darcy Parameter})$$

$$N = \frac{\beta_1^* \Delta C}{\beta_1 \Delta T} \quad (\text{the Buoyancy ratio}) \quad Sc = \frac{\nu}{D_1} \quad (\text{the Schmidt number})$$

$$So = \frac{k_{11} \beta_1^*}{\Delta C} \quad (\text{the Soret parameter})$$

Under these constraints imposed  $\bar{J}$  has only the azimuthally components  $J_\theta$  while  $q$  and  $B$  have axial and radial components.

We assume

$$\bar{q} = (u, v) \quad , \quad \bar{B} = (f, g)$$

The boundary conditions relevant to the problem are

$$\begin{aligned} v(r, x) = 0, \frac{\partial v}{\partial r} = 0, \frac{\partial \theta}{\partial r} = 0, \frac{\partial C}{\partial r} = 0 \quad \text{on } r = 0 \\ u(r, x) = 0, T - T_e = \gamma(\delta x), C = C_1 \quad \text{on } r = a \end{aligned} \quad (2.18)$$

Equations (2.11)-(2.14) constitute a system of six equations for the seven unknowns  $u, v, f, g, J_0, \theta$  and  $C$ . These may be reduced to three equations for the Stoker's stream function  $\psi(r, x)$  and the magnetic stream function  $\phi(r, x)$  given by

$$u = -\frac{1}{r} \frac{\partial \psi}{\partial r}, \quad v = \frac{1}{r} \frac{\partial \psi}{\partial x}$$

$$f = -\frac{1}{r} \frac{\partial \phi}{\partial r}, \quad g = \frac{1}{r} \frac{\partial \phi}{\partial x}$$

(The subscripts  $x$  and  $r$  denote the respective partial derivatives). combining (2.15) and (2.17) to eliminate  $J$ . We find

$$E^2 \phi = R_m \left( \frac{1}{r} \right) (\psi_x \phi_r - \psi_r \phi_x) \quad (2.19)$$

Where the operator  $E^2$  is denoted by

$$E^2 = r \frac{\partial}{\partial r} \left( \frac{1}{r} \frac{\partial}{\partial r} \right) + \frac{\partial^2}{\partial x^2}$$

Eliminating  $J$  between (2.2) and (2.8) and taking the curl of the former to eliminate the pressure, we get

$$R_e \left( \frac{1}{r} \frac{\partial \psi}{\partial x} \frac{\partial (E^2 \psi)}{\partial r} - \frac{1}{r} \frac{\partial \psi}{\partial r} \frac{\partial (E^2 \psi)}{\partial x} - \frac{2}{r^2} \frac{\partial \psi}{\partial x} E^2 \psi \right) - E^2 (E^2 \psi) +$$

$$+ M^2 / R_m \{ (1/r) \phi_x (E^2 \phi)_r - (1/r) \phi_r (E^2 \phi)_x -$$

$$- (2/r^2) \phi_x \{ E^2 \phi \}_r - \{ G / R_e \} (r \left( \frac{\partial \theta}{\partial r} + N \frac{\partial C}{\partial r} \right)) \} \quad (2.20)$$

The energy equation is

$$P_e (\theta_r \psi_x - \theta_x \phi_r) = \theta_{rr} + (1/r) \theta_r + \theta_{xx} + 1 \quad (2.21)$$

The diffusion equation is

$$R_e Sc (C_r \psi_x - C_x \phi_r) = C_{rr} + (1/r) C_r + C_{xx} + \frac{Sc So}{N} (\theta_{rr} + (1/r) \theta_r + \theta_{xx}) \quad (2.22)$$

The current density can be found once  $\psi$  and  $\phi$  are known from equations (2.17) which reduce to

$$J_\theta = (1/r^2) (\psi_x \theta_r - \psi_r \phi) \quad (2.23)$$

These coupled equations (2.17)-(2.19) are to be solved subject to non dimensional boundary conditions.

$$\psi(r, x) = 0, \quad \frac{\partial}{\partial r} \left( (1/r) \frac{\partial \psi}{\partial r} \right) = 0 \quad (2.24)$$

$$\frac{\partial \theta}{\partial r} = 0, \quad \frac{\partial C}{\partial r} = 0 \quad \text{on } r = 0 \quad (2.25)$$

$$\psi(r, x) = -1/2, \quad \frac{\partial \psi}{\partial r} = 0 \quad (2.26)$$

$$\theta(r, x) = \gamma(\delta x), \quad C(r, x) = 1 \quad \text{on } r = f \quad (2.27)$$

The value of  $\psi$  on the boundary assures the constant volumetric flow in consistence with the hypothesis (2.1) and conditions (2.24) & (2.26) corresponds to axial symmetry of the flow.

Electric currents within the fluid induces a magnetic field exterior to the tube as well as within. This external field,

$$\hat{B} = (\hat{f}, \hat{g}) \text{ is given by a potential } \hat{A} = \hat{\phi} e_\theta, \text{ such that}$$

$$\hat{B} = \nabla x \hat{A}, \text{ or}$$

$$\hat{f} = -(1/r) \hat{\phi}_r, \quad \hat{g} = (1/r) \hat{\phi}_x$$

Since  $R_m = 0$  in the exterior region equation (2.18) requires

$$E^2 \hat{\phi} = 0$$

Both the potential and the field itself must be continuous at the wall (7). Hence we may write the matching condition are

$$\phi = \hat{\phi} \quad \text{at} \quad r = f(x)$$

$$\phi_r = \hat{\phi}_r \quad \text{at} \quad r = f(x)$$

The problem statement is completed by boundary conditions at  $r = 0$ ,  $r \rightarrow \pm\infty$ . Because of symmetry the radial field must vanish at the centre line.

$$(1/r) \phi_x = 0 \quad \text{at} \quad r = 0$$

and we must retrieve the uniform applied field both far from the tube,

$$\lim_{r \rightarrow \pm\infty} (1/r) \hat{\phi} = \lim_{x \rightarrow \pm\infty} (1/r) \phi_r = -1$$

On the boundary with variable cross-section  $(1/r) (\partial\phi / \partial r)$  is either a constant or a function  $x$ . Supposing  $\phi_r \neq 0$  then  $f$  is function of  $x$  along the tube. In view of the continuity requirements it follows that in the neighbourhood of the tube at any case  $r$ .

$$\hat{f} = -(1/r) \hat{\phi}_r = -1$$

$$\lim_{r \rightarrow \infty} (1/r) \hat{\phi}_r = -1$$

Therefore  $\hat{\phi}_r \neq 0$  on  $r = f(x)$  leads to a contradiction.

But  $\phi_r = \hat{\phi}_r$  in view of the matching condition on  $r = f(x)$ .

Therefore on  $r = f(x)$ ,  $\phi_r = \hat{\phi}_r = 0$

### 3. Analysis of the flow

We introduce the transformations(11)

$$\bar{x} = \delta x$$

we assume  $\frac{\partial}{\partial x} \approx O(\delta)$  such that  $\frac{\partial}{\partial \bar{x}} \approx O(1)$  for small values of  $\delta$ , the flow develops slowly along the axial direction with gradient  $O(\delta)$ . Making use of the above transformation the equations(2.19)-(2.22) reduce to

$$E_1^2 \phi = \delta R_m \left( \frac{1}{r} \right) (\psi_x \phi_r - \psi_r \phi_x) \quad (3.1)$$

$$\begin{aligned} (\delta R_e) \left( \frac{1}{r} \frac{\partial \psi}{\partial \bar{x}} \frac{\partial (E_1^2 \psi)}{\partial r} - \frac{1}{r} \frac{\partial \psi}{\partial r} \frac{\partial (E_1^2 \psi)}{\partial \bar{x}} - \frac{2}{r^2} \frac{\partial \psi}{\partial \bar{x}} E_1^2 \psi \right) - E_1^4 \psi + \\ + M^2 / R_m \{ (1/r) \phi_{\bar{x}} (E_1^2 \phi)_r - (1/r) \phi_r (E_1^2 \phi)_{\bar{x}} - \\ - (2/r^2) \phi_{\bar{x}} \{ E_1^2 \phi \}_r \} - \{ G / R_e \} \left( r \left( \frac{\partial \theta}{\partial r} + N \frac{\partial C}{\partial r} \right) \right) \end{aligned} \quad (3.2)$$

$$(\delta P_e) (\theta_r \psi_{\bar{x}} - \theta_x \phi_r) = \theta_{rr} + (1/r) \theta_r + \delta^2 \theta_{xx} + 1 \quad (3.3)$$

$$((\delta R_e S c) (C_r \psi_{\bar{x}} - C_{\bar{x}} \phi_r)) = C_{rr} + (1/r) C_r + \delta^2 C_{xx} + \frac{Sc So}{N} (\theta_{rr} + (1/r) \theta_r + \delta^2 \theta_{xx}) \quad (3.4)$$

Where

$$E_1^2 = r \frac{\partial}{\partial r} \left( \frac{1}{r} \frac{\partial}{\partial r} \right) + \delta^2 \frac{\partial^2}{\partial \bar{x}^2}$$

Assume  $R_e \approx O(1)$  in the limit  $\delta \rightarrow 0$  the inertial terms vanish in equations(3.2) leading the viscous terms and the magnetic terms. The order of the magnetic term depends on  $M$  as well as  $\delta$ . From equation (3.1) we find that  $E_1^2 \phi \approx O(\delta)$  for  $R_m \approx O(1)$ . Thus we may consider the Hartmann number  $M$  as large as  $O(\delta^{-1/2})$  and still

retain only the viscous terms at the zeroth order with both inertial and magnetic perturbations appearing in first order. Thus we elevate magnetic effects to first order neglecting the second order inertial and viscous effects . Taking the transformation

$$\eta = \frac{r}{f(\bar{x})}$$

the above equations reduce to

$$F^2 \phi = (\delta f R_m) \left( \frac{1}{\eta} \right) (\psi_x \phi_\eta - \psi_\eta \phi_x) \quad (3.5)$$

$$\begin{aligned} (\delta f R_e) \left( \frac{1}{\eta} \frac{\partial \psi}{\partial \bar{x}} \frac{\partial (F^2 \psi)}{\partial \eta} - \frac{1}{\eta} \frac{\partial \psi}{\partial \eta} \frac{\partial (F^2 \psi)}{\partial \bar{x}} - \frac{2}{\eta^2} \frac{\partial \psi}{\partial \bar{x}} F^2 \psi \right) - F^4 \psi + \\ + (f \hat{M}^2 / R_m) \{ (1/\eta) \phi_{\bar{x}} F^2 \phi \}_\eta - (1/\eta) \phi_\eta (F^2 \phi)_{\bar{x}} - \\ - (2/\eta^2) \phi_{\bar{x}} \{ F \phi \}_\eta - \{ Gf^4 / R_e \} \left( \eta \left( \frac{\partial \theta}{\partial \eta} + N \frac{\partial C}{\partial \eta} \right) \right) \end{aligned} \quad (3.6)$$

$$(\delta f P_e) (\theta_\eta \psi_{\bar{x}} - \theta_x \phi_\eta) = \theta_{\eta\eta} + (1/\eta) \theta_\eta + \delta^2 f^2 \theta_{xx} + f^2 \quad (3.7)$$

$$\begin{aligned} (\delta R_e f Sc) (C_\eta \psi_{\bar{x}} - C_{\bar{x}} \psi_\eta) = C_{\eta\eta} + (1/\eta) C_\eta + \delta^2 f^2 C_{xx} + \\ + \frac{Sc So}{N} (\theta_{\eta\eta} + (1/\eta) \theta_\eta + \delta^2 f^2 \theta_{xx}) \end{aligned} \quad (3.8)$$

where

$$F^2 = \eta \frac{\partial}{\partial \eta} \left( \frac{1}{\eta} \frac{\partial}{\partial \eta} \right)$$

We use the asymptotic expansions

$$\begin{aligned} \psi(\eta, \bar{x}) &= \psi_0(\eta, \bar{x}) + \delta \psi_1(\eta, \bar{x}) + \delta^2 \psi_2(\eta, \bar{x}) + \dots \\ \theta(\eta, \bar{x}) &= \theta_0(\eta, \bar{x}) + \delta \theta_1(\eta, \bar{x}) + \delta^2 \theta_2(\eta, \bar{x}) + \dots \\ C(\eta, \bar{x}) &= C_0(\eta, \bar{x}) + \delta C_1(\eta, \bar{x}) + \delta^2 C_2(\eta, \bar{x}) + \dots \\ \phi(\eta, \bar{x}) &= \phi_0(\eta, \bar{x}) + \delta \phi_1(\eta, \bar{x}) + \delta^2 \phi_2(\eta, \bar{x}) + \dots \end{aligned} \quad (3.9)$$

Substituting (3.9) in equations(3.5)-(3.8) and separating the like powers of  $\delta$  ,the equations corresponding to the zeroth order are

$$\theta_{0,\eta\eta} + \frac{1}{\eta} \theta_{0,\eta} + f^2 = 0 \quad (3.10)$$

$$C_{0,\eta\eta} + \frac{1}{\eta} C_{0,\eta} = -\frac{Sc So}{N} (\theta_{0,\eta\eta} + \frac{1}{\eta} \theta_{0,\eta}) \quad (3.11)$$

$$F^4 \psi_0 - h^2 F^2 \psi_0 + \frac{Gf^4}{R_e} (\eta (\theta_{0,\eta} + N C_{0,\eta})) = 0 \quad (3.12)$$

$$F^2 \phi_0 = 0 \quad (3.13)$$

The corresponding conditions on  $\psi_0$ ,  $\theta_0$ ,  $C_0$  and  $\phi_0$  are

$$\begin{aligned} \psi_0(1, \bar{x}) = -1/2, \quad (\psi_{0,\eta})_{\eta=1} = 0 \\ (\eta \psi_{0,\eta\eta} - \psi_{0,\eta})_{\eta=0} = 0, \quad \psi_0(0, \bar{x}) = 0 \end{aligned} \quad (3.14a)$$

$$\theta_0(1, \bar{x}) = \gamma(\bar{x}), \quad (\theta_{0,\eta})_{\eta=0} = 0 \quad (3.14b)$$

$$C_0(1, \bar{x}) = 0, \quad (C_{0,\eta})_{\eta=0} = 0 \quad (3.14c)$$

$$\phi_{0,x}(0, \bar{x}) = 0, \quad \lim_{r \rightarrow \infty} \left( \frac{1}{r} \phi_{0,\eta} \right) = -1 \quad (3.14d)$$

The equations to the first order are

$$\eta \theta_{1,\eta\eta} + \theta_{1,\eta} = P_e (\psi_{0,\bar{x}} \theta_{0,\eta} - \psi_{0,\eta} \theta_{0,\bar{x}}) \quad (3.15)$$

$$\eta C_{1,\eta\eta} + C_{1,\eta} = R_e Sc (\psi_{0,\bar{x}} C_{0,\eta} - \psi_{0,\eta} C_{0,\bar{x}}) - \frac{ScSo}{N} (\eta \theta_{1,\eta\eta} + \theta_{1,\eta}) \quad (3.16)$$

$$F^2 (F^2 - h^2) \psi_1 = f^4 R_e (\psi_{0,\bar{x}} (F^2 \psi_0)_\eta - \psi_{0,\eta} (F^2 \psi_0)_{\bar{x}} - \left( \frac{2}{r^2} \right) \psi_{0,\bar{x}} (F^2 \psi_0)) - \hat{M}^2 f^4 / R_m (\phi_{0,\bar{x}} (F^2 \phi_0)_\eta) \quad (3.17)$$

$$- \phi_{0,\eta} (F^2 \phi_0)_{\bar{x}} - \left( \frac{2}{r^2} \right) \phi_{0,\bar{x}} (F^2 \phi_0)) + \frac{Gf^4}{R_m} (\eta (\theta_{1,\eta} + NC_{1,\eta}))$$

$$F^2 \phi_1 = R_m (\psi_{0,\bar{x}} \phi_{0,\eta} - \psi_{0,\eta} \phi_{0,\bar{x}}) \quad (3.18)$$

Where

$$\hat{M}^2 = \delta M^2 \cong O(1), \quad h^2 = D^{-1} f^2$$

The corresponding conditions on  $\psi_1$ ,  $\theta_1$ ,  $C_1$  and  $\phi_1$  are

$$\psi_1(1, \bar{x}) = -0, \quad (\psi_{1,\eta})_{\eta=1} = 0$$

$$(\eta \psi_{1,\eta\eta} - \psi_{1,\eta})_{\eta=0} = 0, \quad \psi_1(0, \bar{x}) = 0 \quad (3.19a)$$

$$\theta_1(1, \bar{x}) = \gamma(\bar{x}), \quad (\theta_{1,\eta})_{\eta=0} = 0 \quad (3.19b)$$

$$C_1(1, \bar{x}) = 0, \quad (C_{1,\eta})_{\eta=0} = 0 \quad (3.19c)$$

$$\phi_{1,x}(0, \bar{x}) = 0, \quad \phi_{1,\eta} = \hat{\phi}_{1,\mu} = 0 \quad \text{on } \eta = 1 \quad (3.19d)$$

The equations to the second order are

$$\eta \theta_{2,\eta\eta} + \theta_{2,\eta} = P_e (\psi_{0,\bar{x}} \theta_{1,\eta} - \psi_{0,\eta} \theta_{1,\bar{x}} + \psi_{1,\bar{x}} \theta_{0,\eta} - \psi_{1,\eta} \theta_{0,\bar{x}}) \quad (3.20)$$

$$\eta C_{2,\eta\eta} + C_{2,\eta} = R_e Sc (\psi_{0,\bar{x}} C_{1,\eta} - \psi_{0,\eta} C_{1,\bar{x}} + \psi_{1,\bar{x}} C_{0,\eta} - \psi_{1,\eta} C_{0,\bar{x}}) - \frac{ScSo}{N} (\eta \theta_{2,\eta\eta} + \theta_{2,\eta}) \quad (3.21)$$

$$F^2 (F^2 - h^2) \psi_2 = f^4 R_e (\psi_{1,\bar{x}} (F^2 \psi_0)_\eta - \psi_{0,\eta} (F^2 \psi_1)_{\bar{x}} - \left( \frac{2}{r^2} \right) (\psi_{0,\bar{x}} (F^2 \psi_1) + \psi_{1,\bar{x}} (F^2 \psi_0)) - \psi_{0,\bar{x}} (F^2 \psi_1)_\eta - \psi_{1,\eta} (F^2 \psi_0)_{\bar{x}} - \hat{M}^2 f^4 / R_m (\phi_{0,\bar{x}} (F^2 \phi_0)_\eta - \phi_{0,\eta} (F^2 \phi_0)_{\bar{x}}) - \left( \frac{2}{r^2} \right) \phi_{0,\bar{x}} (F^2 \phi_0)) + \frac{Gf^4}{R_m} (\eta (\theta_{1,\eta} + NC_{1,\eta})) \quad (3.22)$$

$$- \psi_{1,\eta} (F^2 \psi_0)_{\bar{x}} - \hat{M}^2 f^4 / R_m (\phi_{0,\bar{x}} (F^2 \phi_0)_\eta - \phi_{0,\eta} (F^2 \phi_0)_{\bar{x}}) - \left( \frac{2}{r^2} \right) \phi_{0,\bar{x}} (F^2 \phi_0)) + \frac{Gf^4}{R_m} (\eta (\theta_{1,\eta} + NC_{1,\eta}))$$

$$F^2 \phi_2 = f R_m (\psi_{0,\bar{x}} \phi_{1,\eta} - \psi_{0,\eta} \phi_{1,\bar{x}} + \psi_{1,\bar{x}} \phi_{0,\eta} - \psi_{1,\eta} \phi_{0,\bar{x}}) \quad (3.23)$$

The corresponding conditions on  $\psi_2$ ,  $\theta_2$ ,  $C_2$  and  $\phi_2$  are

$$\psi_2(1, \bar{x}) = -0, \quad (\psi_{2,\eta})_{\eta=1} = 0$$

$$(\eta \psi_{2,\eta\eta} - \psi_{2,\eta})_{\eta=0} = 0, \quad \psi_2(0, \bar{x}) = 0 \quad (3.24a)$$

$$\theta_2(1, \bar{x}) = 0, \quad (\theta_{2,\eta})_{\eta=0} = 0 \quad (3.24b)$$

$$C_2(1, \bar{x}) = 0, \quad (C_{2,\eta})_{\eta=0} = 0 \quad (3.24c)$$

$$\phi_{2,x}(0, \bar{x}) = 0, \quad \phi_{2,\eta} = \hat{\phi}_{2,\mu} = 0 \quad \text{on } \eta = 1 \quad (3.24d)$$

where

$$F^2 = \frac{\partial^2}{\partial \eta^2} - \frac{1}{\eta} \frac{\partial}{\partial \eta}$$

**4. Solution of the problem**

Solving the coupled equations (3.10)-(3.13) subject to the corresponding boundary conditions (3.14a)-(3.14d), we get the expressions for zeroth order

$$\theta_0(\bar{x}, \eta) = \gamma(\bar{x}) - f^2(1 - \eta^2) / 4$$

$$C_o = a_1(1 - \eta^2) / 4$$

$$\psi_0 = a_5 + \frac{a_4}{4} \eta^2 - \frac{a_3}{360} \eta^6$$

$$\phi_0 = -\frac{\eta^2}{2}$$

Solving the coupled equations (3-15)-(3,18) subject to the corresponding conditions(3,19a)-(3,19d), the solution for  $\theta_1, C_1, \psi_1$  and  $\phi_1$  are

$$\begin{aligned} \theta_1 &= \frac{a_9}{9}(\eta^3 - 1) + \frac{a_{10}}{25}(\eta^5 - 1) + \frac{a_{11}}{49}(\eta^7 - 1) - \frac{a_{12}}{81}(\eta^9 - 1) \\ C_1 &= \frac{a_{15}}{6}(\eta^2 - 1) + \frac{a_{16}}{16}(\eta^4 - 1) + \frac{a_{17}}{25}(\eta^5 - 1) + \frac{a_{18}}{49}(\eta^7 - 1) + \frac{a_{19}}{64}(\eta^9 - 1) + \frac{a_{30}}{81}(\eta^{10} - 1) \\ \phi_1 &= \frac{a_{21}}{4} \eta^2 + \frac{a_{22}}{9} \eta^3 + \frac{a_{33}}{25} \eta^5 + \frac{a_{24}}{64} \eta^8 + \frac{a_{25}}{81} \eta^9 \\ \psi_1 &= \frac{a_{61}}{9} \eta^3 + \frac{a_{62}}{180} \eta^5 + \frac{a_{63}}{576} \eta^6 + \frac{a_{64}}{1225} \eta^7 + \frac{a_{65}}{(36 \times 64)} \eta^8 + \frac{a_{66}}{(49 \times 81)} \eta^9 \\ &+ \frac{a_{67}}{6400} \eta^{10} + \frac{a_{68}}{(81 \times 21)} \eta^{11} + \frac{a_{69}}{14400} \eta^{12} + \frac{a_{70}}{(160 \times 121)} \eta^{13} + \frac{a_{71}}{(144 \times 189)} \eta^{14} \\ &+ \frac{B_1}{2} \eta^2 + B_2 \end{aligned}$$

where  $a_1, a_2, \dots, a_{71}, B_1, B_2$  are constants.

The stress tensor for the motion on the pipe

$$\sigma_{ij} = -p\delta_{ij} + 2\rho v e_{ij}$$

Where

$$e_{xx} = \frac{\partial u}{\partial x}, e_{rr} = \frac{\partial v}{\partial r}$$

$$e_{rx} = 0.5\left(\frac{\partial u}{\partial r} + \frac{\partial v}{\partial x}\right)$$

The shear stress on the pipe  $r=f(x)$ , in the non-dimensional form is given by

$$\tau = (\sigma_{rx}(1 - f'^2) + (\sigma_{rr} - \sigma_{xx})f' / (1 + f'^2))$$

In terms of non-dimensional variables, we obtain the non-dimensional shear stress is

$$\begin{aligned} \tau &= \left(\frac{P_1}{2f^3} \left( (P_2 \left( \frac{1}{\eta^2} \right) \psi_{0,\eta} - \frac{1}{\eta} \psi_{0,\eta\eta} \right) + \epsilon \left( P_2 \left( \frac{1}{\eta^2} \right) \psi_{1,\eta} - \frac{1}{\eta} \psi_{1,\eta\eta} \right) \right. \right. \\ &\left. \left. + 2ff' \left( \left( \frac{2}{\eta} \right) \psi_{0,r\eta} - \left( \frac{1}{\eta^2} \right) \psi_{0,x} \right) \right) \right) \end{aligned}$$

where

$$P_1 = \frac{1}{1 + f'^2}, P_2 = 1 - f'^2$$

The local rate of heat transfer coefficient(Nusselt number) on the boundary of the pipe is calculated using the formula

$$Nu = \frac{1}{f(\theta_m - \theta_w)} \left( \frac{\partial \theta}{\partial \eta} \right)_{\eta=1}$$

where

$$\theta_m = 2 \int_0^1 \theta d\eta$$

and the corresponding expression is

$$Nu = \frac{B_{17} + \delta B_{18}}{f(B_{15} + \delta B_{16} - \gamma(\bar{x}))}$$

The local rate mass transfer coefficient (Sherwood Number)on the boundary of the pipe is calculated using the formula

$$Sh = \frac{1}{f(C_m - C_w)} \left( \frac{\partial C}{\partial \eta} \right)_{\eta=1}$$

where

$$C_m = 2 \int_0^1 C d\eta$$

and the corresponding expression is

$$Sh = \frac{B_{23} + \delta B_{24}}{f(B_{21} + \delta B_{24})}$$

where B<sub>1</sub>,B<sub>2</sub>,.....B<sub>24</sub> are constants.

### 5. Discussion of the numerical results

The aim of the analysis is study the effect of the non-uniform temperature on the flow, heat and mass transfer of a viscous, electrically conducting fluid in a non-uniform pipe in the presence of a constant heat source/ sink. The coupled equations governing the flow, heat and mass transfer have been solved using a perturbation technique . The velocity, the temperature and the concentration distributions in the fluid region are analytically evaluated and their behavior w.r.t variations in the governing parameters G, R, M, Sc, S<sub>0</sub>,α and N has been analysed numerically. For computational purpose the geometry of the pipe wall in the non-dimensional form is assumed to be  $r = f(\bar{x}) = 1 + \beta e^{-x^2}$  and the prescribed wall temperature  $\gamma(\bar{x})$  is chosen to be  $\alpha \sin(\bar{x})$ ,  $\beta > 0$  corresponds to the dilation of the pipe and  $\beta < 0$  corresponds to the constriction of the pipe. In this analysis we confine our study to a constricted pipe. We note that the Grashof number G is positive or negative according as the equilibrium temperature on the boundary is less than or greater than the actual temperature. The Reynolds number R<sub>m</sub> is chosen to be 10. This R<sub>m</sub>( $> 1$ ) being finite the induced magnetic field can not be neglected in comparison to the applied field and thus influences the flow to a certain extent. In view of the magnetic flux condition the current density vector.  $\bar{J}$  is expressible in terms of the magnetic stream function  $\phi$  and hence the governing equations are coupled equations involving  $\psi$ ,  $\phi$ ,  $\theta$  and C. The equations are uncoupled under a perturbation scheme and using the ohm's law and the perturbation parameter is chosen to be the slope of the non - uniform pipe. Hence basically we assume that the flow variables vary slowly along the axial direction of the pipe. Figs.(1)-(15) give the profiles of u and v for different parametric values in a constricted pipe. We note that the actual flow due to imposed flux and the pressure gradient is positive, along the x-axis and hence negative axial velocity corresponds to the reversal flow. Such reversal flows are consequences of thermal buoyancy and molecular buoyancy and give rise to convection cells. It is interesting to observe that the geometry of the boundary has direct influence on the occurrence of these convection cells. Fig.1 shows that the reversal flow appears in the entire fluid region for all  $G > 0$  and no such reversal flow appears for  $G < 0$  .The region of reversal flow increases in its size with increase in G and the magnitude of u increases with  $|G|$  (<or>).Fig.9 shows the variation of the secondary velocity v with G in a constricted pipe. It is found that for every  $G > 0$  and  $|G| = 10^3$ , v is towards the boundary while for  $|G| > 3 \times 10^3$  it is towards the midregion.The magnitude of v however increases with  $G > 0$  while an increase in  $|G| \leq 3 \times 10^3$ , v experiences a reduction in its magnitude and for further increase in  $|G|$  we find an enhancement in  $|v|$ .Also  $|u|$  and

$|v|$  decrease with  $R$  in the entire fluid region. An increase in  $M$  reduces  $|u|$  and enhances  $|v|$  (fig.2&10). The variation of  $u$  and  $v$  with  $Sc$  shows that lesser the molecular diffusivity smaller the magnitude of  $u$  and larger the magnitude of  $v$  in the entire fluid region (fig.3&11). The influence of Soret parameter ( $S_0$ ) on  $u$  and  $v$  indicates that when  $S_0$  increases through positive values we find the disappearance of reversal flow in the fluid region while  $S_0$  increases through negative values we find an reversal flow in the region with increase in its size. The magnitude of  $u$  decreases with  $S_0 < 0$  and increases with  $S_0 > 0$  and  $v$  enhances with increase in  $|S_0|$  ( $< \text{or} > 0$ ) (fig.12). The buoyancy ratio ( $N$ ) measures the ratio the molecular buoyancy force and the thermal buoyancy force. When the molecular buoyancy force dominates over the thermal buoyancy force  $|u|$  enhances when the buoyancy forces are in the same direction and it experiences a reduction when they act in opposite directions (fig.5). The secondary velocity  $v$  is towards the boundary irrespective of the directions of the buoyancy forces. We find that  $v$  reduces with  $N$  when the two forces are in the same direction while it experiences a marginal increase with  $N$  when they act in opposite directions (fig.12). The variation of  $u$  and  $v$  with amplitude  $\alpha$  of the prescribed boundary temperature  $\gamma(x)$  are shown in figs.6&13. We find that  $|u|$  experiences a depreciation in its magnitude for an increase in  $\alpha$  (fig.6). The secondary velocity  $v$  reduces with increase in  $\alpha \leq 0.3$  and enhances for higher values of  $\alpha \geq 0.7$  and again decreases for  $\alpha = 1.5$ . The historic behaviour in  $v$  is due to the sinusoidal variation of the boundary temperature. Figs.7&14 indicates the profiles of  $u$  and  $v$  with increase in the amplitude  $\beta$  of the boundary curve. It is found that the velocity  $u$  enhances remarkably with an increase in  $|\beta|$ . An increase in  $|\beta|$  through smaller values decreases  $|v|$  and for higher values of  $|\beta|$ . We find an enhancement in  $|v|$ . Also for higher values of  $|\beta| \geq 1.5$  the velocity  $v$  is towards the midregion for while for smaller values it is towards the boundary (fig.14). Thus higher the constriction of the pipe larger the magnitude of  $u$  and  $v$ . The variation of  $u$  and  $v$  with axial distance  $x$  are shown in figs.8&15. It is found that  $u$  decreases  $v$  increases as we move along the axial distances.

The temperature distribution ( $\theta$ ) is exhibited in figures (16)-(22) for different variations in governing parameters  $G, R, M, Sc, S_0, N, \alpha, \beta$  and  $x$ . It is found that  $\theta$  is positive for all variations. This implies that the actual temperature is greater than the equilibrium temperature in the fluid region. When  $G$  is positive the temperature decreases and it increase for  $G$  negative. (fig.16). An increase in  $R$  enhances  $\theta$  while an increase in  $M$  reduces it in the entire fluid region except in the vicinity of the midregion where it experiences an enhancement (fig.17). The variation of  $\theta$  with  $Sc$  indicates that lesser the molecular diffusivity higher the temperature in the fluid region. (fig.18). The influence of the buoyancy ratio  $N$  on  $\theta$  shows that when the molecular buoyancy force dominates over the thermal buoyancy  $\theta$  reduces when the two forces act in the same direction while it depreciates when they act in opposite directions (fig.19). An increase in  $S_0$  through positive values reduces  $\theta$  while an increase in  $S_0$  through negative values enhances  $\theta$  in the entire fluid region (fig.20). The influence of the amplitude  $\alpha$  of the boundary temperature on  $\theta$  is to depreciates it marginally. The variation of  $\theta$  with amplitude  $|\beta|$  of the constricted pipe shows that  $\theta$  enhances with  $|\beta|$ . Thus we find that higher the constriction of the pipe larger the temperature in the fluid region (fig.22). From fig.22a it is observed that the temperature fluctuates in magnitude as we move along the axial direction.

The concentration distribution ( $C$ ) is exhibited in figures (23) – (31) for different variations of the parameters. It is found that, the concentration  $C$  is positive for all variations. This indicates that the actual concentration is greater than the equilibrium concentration. From fig.23 it is found that an increase in  $G > 0$  enhances the concentration marginally, while for an increase in  $|G|$  ( $< 0$ ) we notice a marginal reduction in  $C$  in the entire fluid region. An enhancement in either  $R$  or  $M$  leads to an depreciation in  $C$  (fig.24&25). From fig.26 we find that when  $Sc$  increases through smaller values of  $Sc$  we find a depreciation in  $C$  while for higher values of  $Sc \geq 1.3$  the concentration increases in the entire fluid region. The variation of  $C$  with  $N$  shows that the concentration experience a depreciation with increase in  $N$  when the two buoyancy forces act in the same direction while a reversed effect is noticed when they act in opposite directions. An increase in  $S_0$  through positive values enhances  $C$  and for negative variation we observe a reduction in  $C$  (fig.28). The influence of non-uniform temperature enhances  $C$  in the entire fluid region. From fig.30 it is found that for greater constriction  $|\beta| \leq 0$ . Also as move along the axial distance the concentration increases with  $x \leq \pi/3$  and decreases for  $x \geq \pi/2$  (fig.31). The average Nusselt number ( $Nu$ ) which measures the rate of heat transfer on  $\eta=1$  is exhibited in tables. It is found that the rate of heat transfer at the boundary is negative for all variations, irrespective of the directions of the buoyancy forces. It is found that the Nusselt number experiences a reduction with increase in  $G > 0$  and an enhancement with  $|G|$  ( $< 0$ ). An increase in  $R$  or  $M$  enhances  $|Nu|$ . Lesser the molecular diffusivity greater the magnitude of  $Nu$  and for further lowering the molecular diffusivity we find a marginal decrease in  $Nu$ . An increase in  $|S_0|$  ( $>$  or  $< 0$ ), reduces  $|Nu|$ . Also  $|Nu|$  reduces with  $|N|$  ( $>$  or  $< 0$ ) irrespective of the directions of the buoyancy forces.  $|Nu|$  experiences a marginal decrease in  $|Nu|$  for  $G > 0$  and an enhancement for  $|G|$  ( $< 0$ ). We find that greater the constriction of the boundary, smaller the rate of heat transfer. As we move along the axial distance we notice a marginal increment in  $Nu$ .



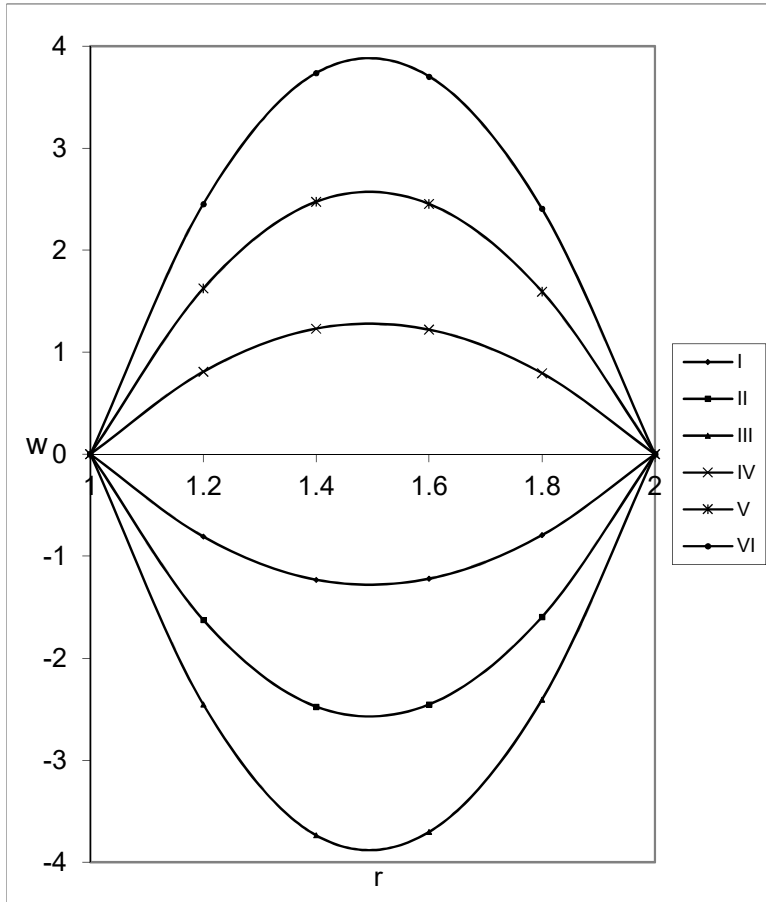


Fig.1 Variation of axial velocity( $w$ ) with  $G$   
 $M=2, D^{-1}=2 \times 10^3, \alpha=2, N=1, Sc=1.3, S_0=0.5$

	I	II	III	IV	V	VI
$G$	$10^3$	$3 \times 10^3$	$5 \times 10^3$	$-10^3$	$-5 \times 10^3$	$-5 \times 10^3$

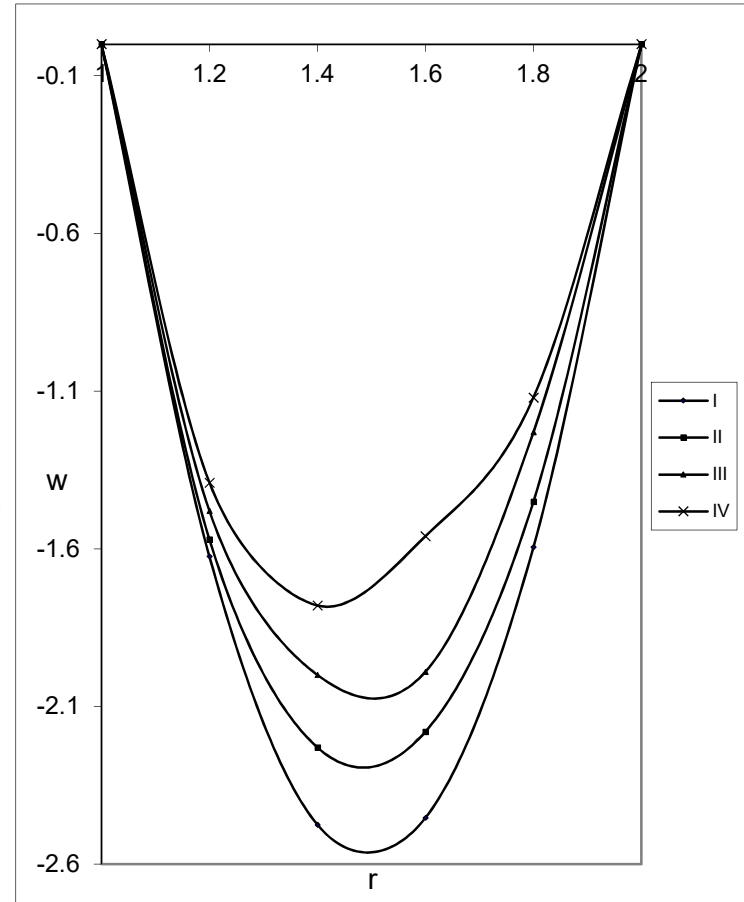


Fig.2  $w$  with  $D^{-1}$

$G=3 \times 10^3, M=2, \alpha=2$

	I	II	III	IV
$D^{-1}$	$10^3$	$3 \times 10^3$	$5 \times 10^3$	$10^4$

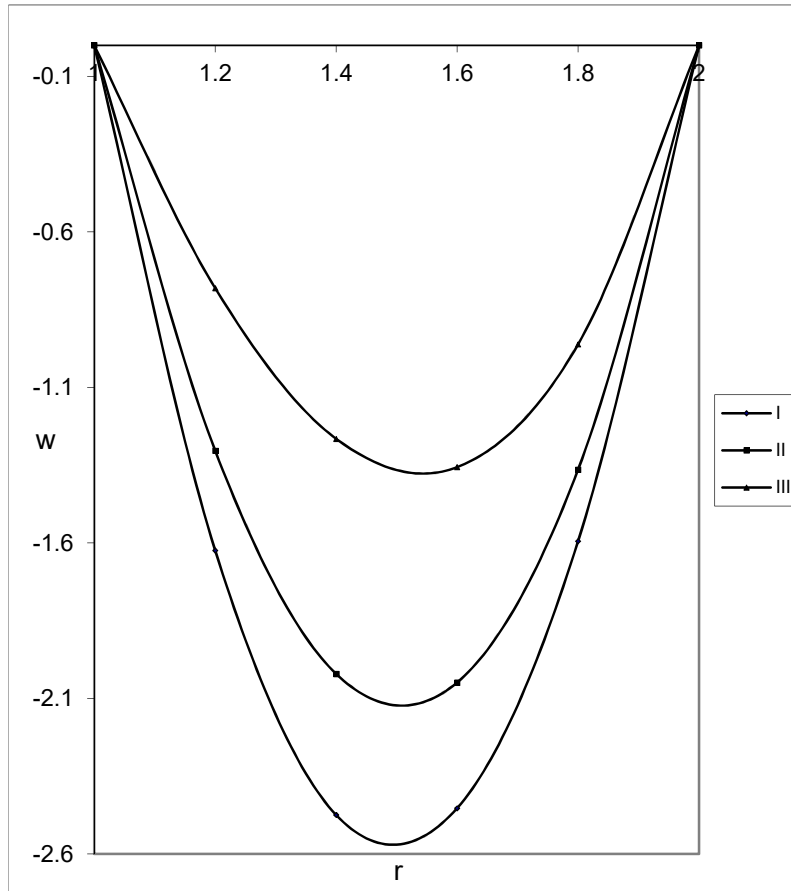


Fig.3 w with M  
 $G = 3 \times 10^3, D^{-1} = 10^3, \alpha = 2$

	I	II	III
M	2	3	5

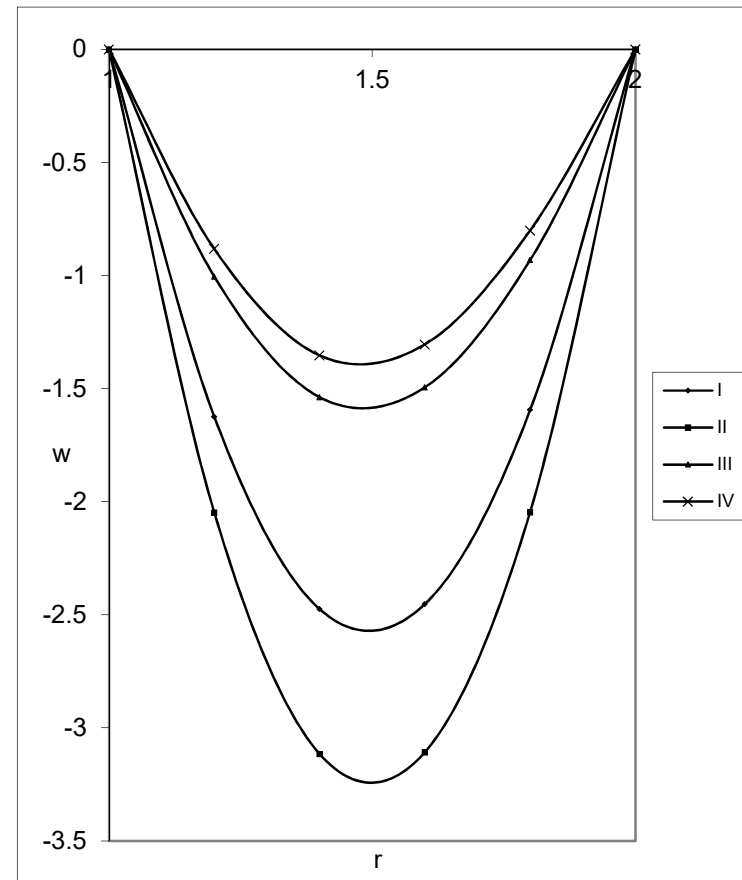


Fig.4 w with N  
 $G = 3 \times 10^3, D^{-1} = 10^3, M = 2, \alpha = 2$

	I	II	III	IV
N	1	2	-0.5	-0.8

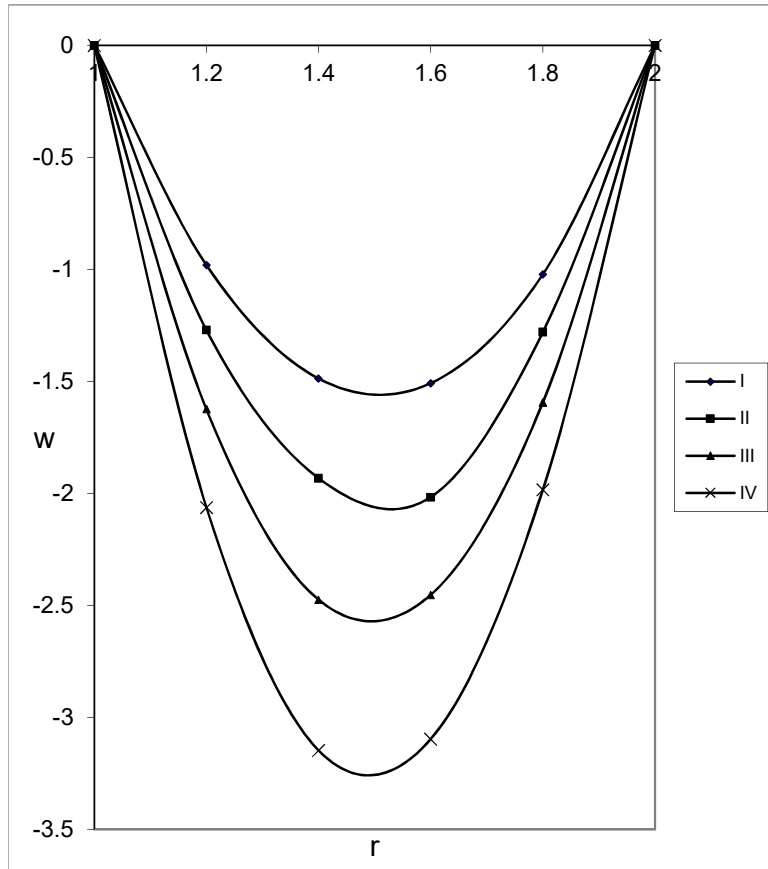


Fig.5 w with Sc

	I	II	III	IV
Sc	0.24	0.6	1.3	2.01

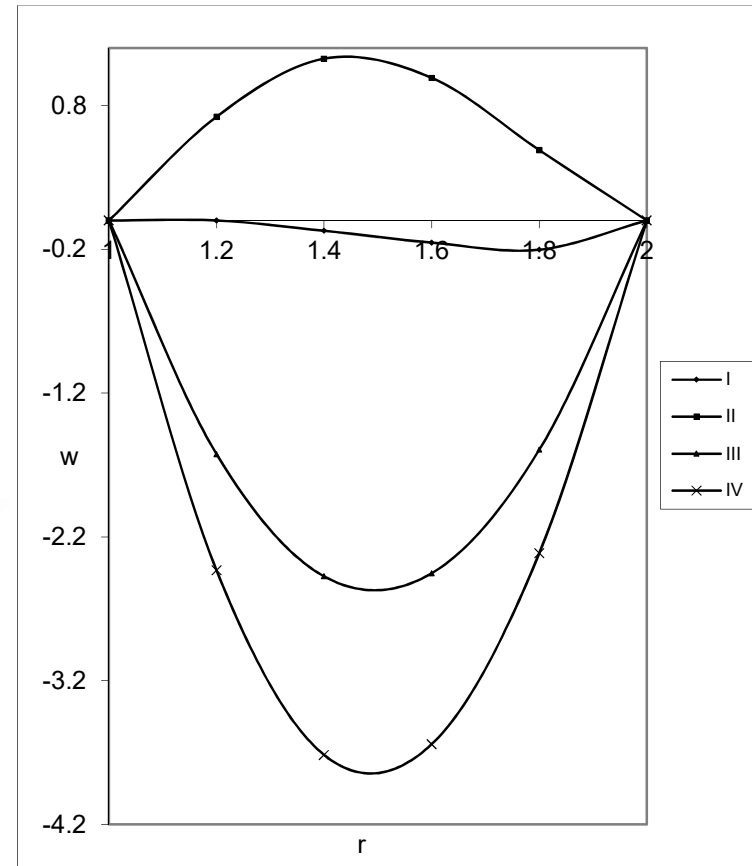


Fig.6 w with  $S_0$   
 $Sc=1.3, N=1, M=2, \alpha=2$

	I	II	III	IV
$S_0$	0.5	1.0	-0.5	-1.0

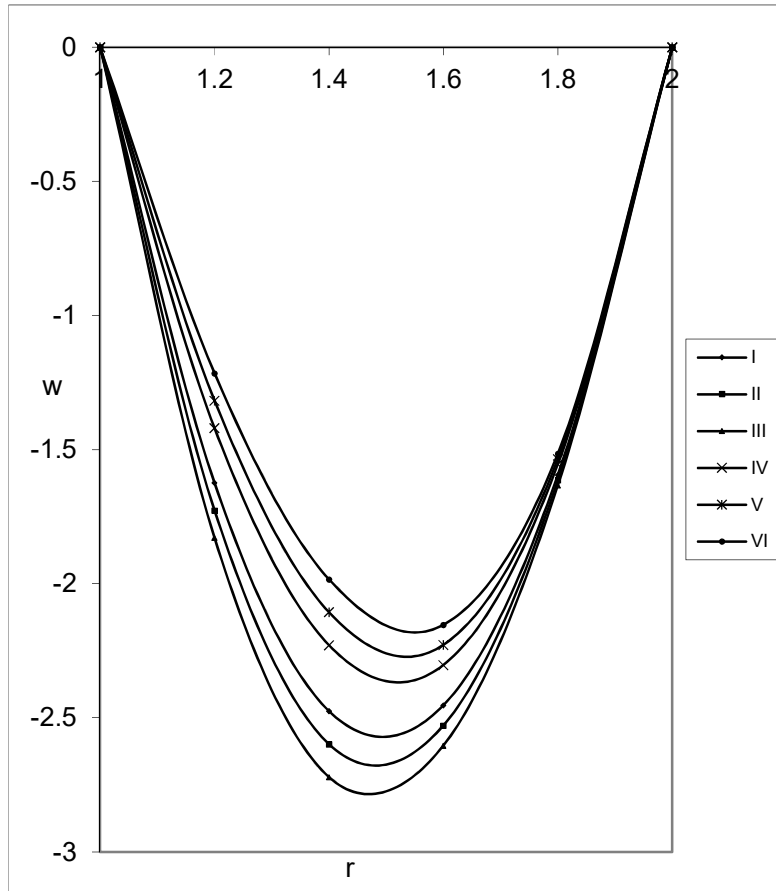


Fig.7  $w$  with  $\alpha$   
 $N=1, Sc=1.3, Sc=0.3, M=2$   
 I II III IV V VI

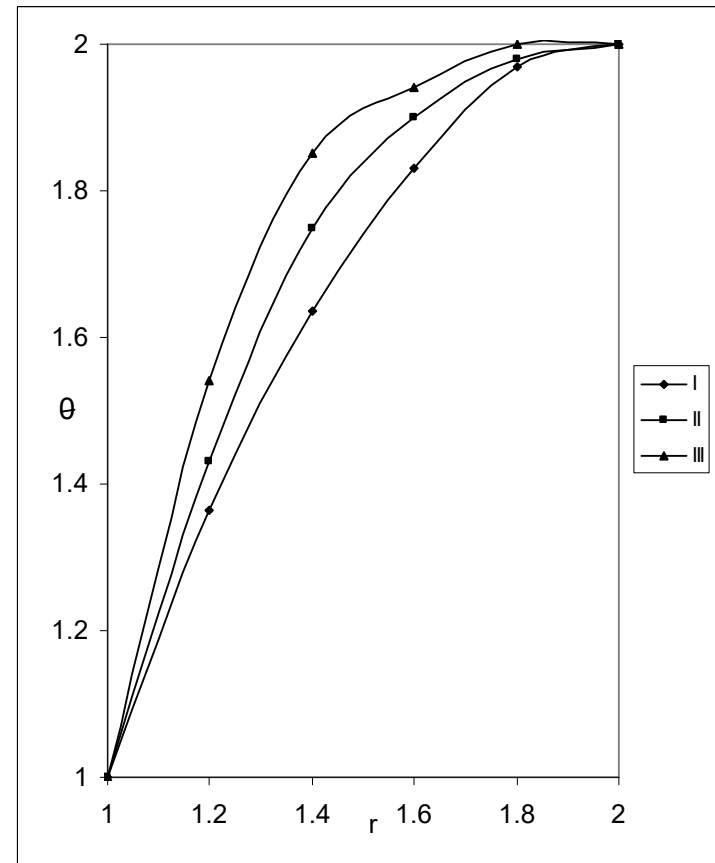


Fig.8 Variation of temperature( $\theta$ ) with  $G$   
 $D^{-1}=10^3, M=2, \alpha=2, N=1, Sc=1.3$   
 I II III

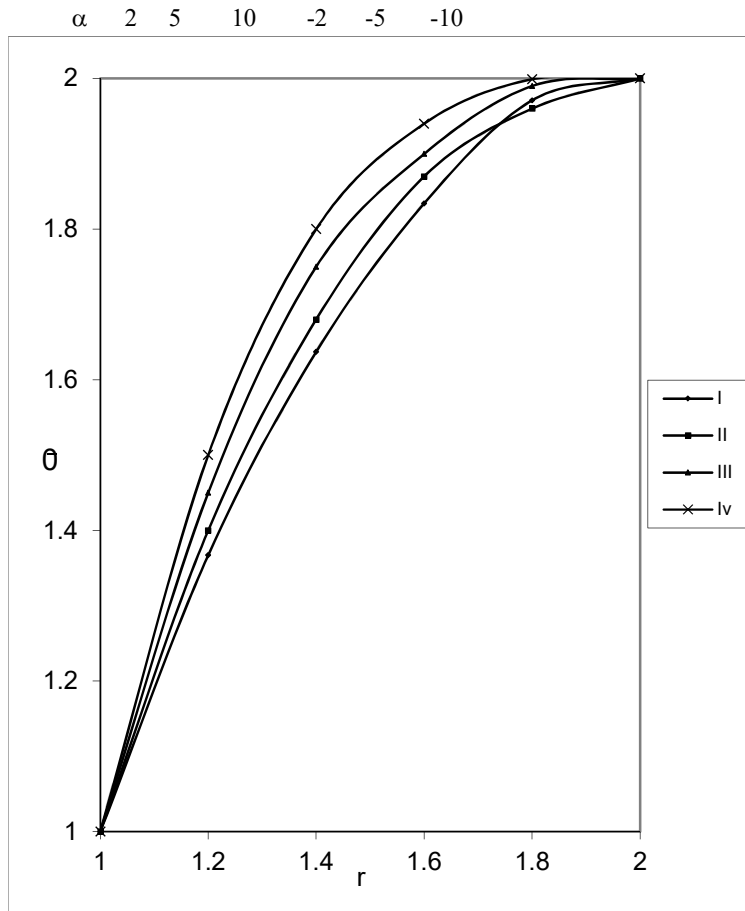


Fig.9  $\theta$  with  $D^{-1}$   
 I II III IV  
 $D^{-1}$   $10^3$   $3 \times 10^3$   $5 \times 10^3$   $10^4$

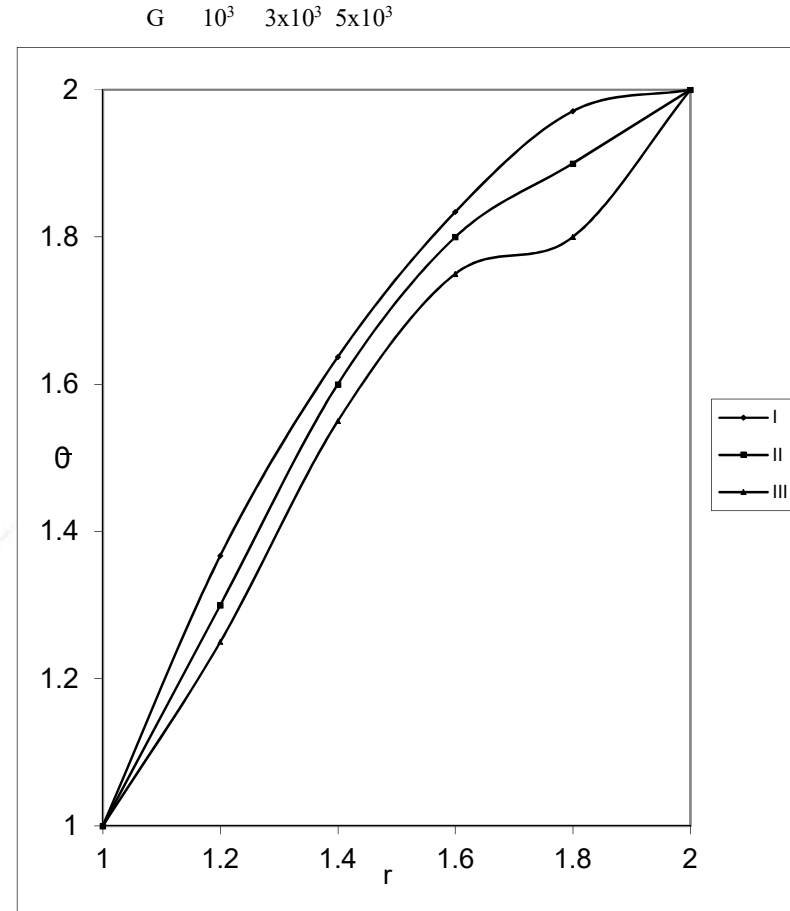


Fig.10  $\theta$  with M  
 I II III  
 M 2 3 5

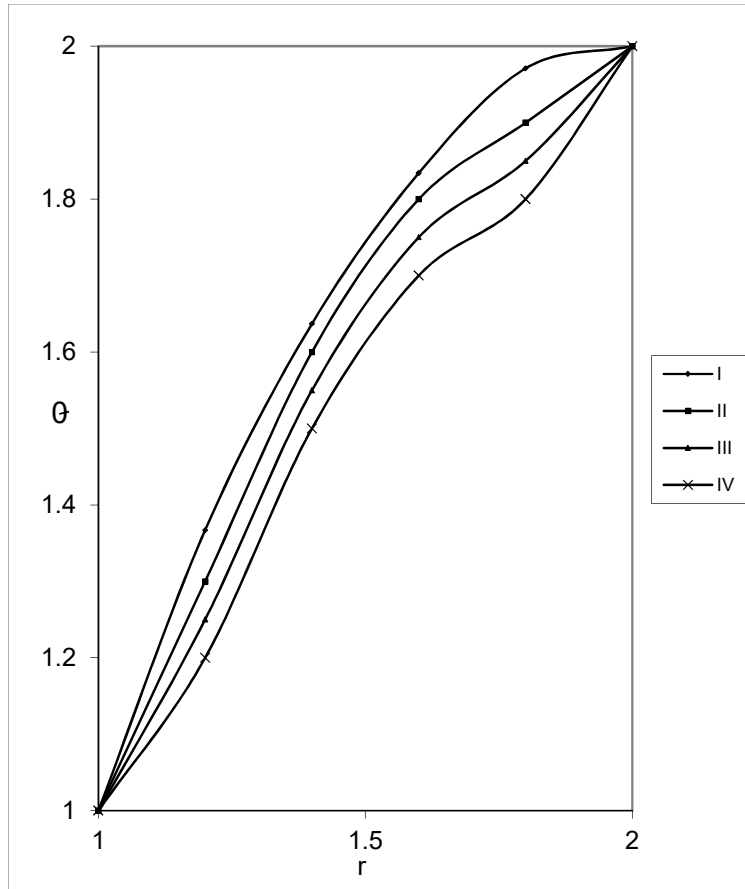


Fig.11  $\theta$  with N  
 $G=3 \times 10^3, D^{-1}=10^3, M=2, \alpha=2$   
 I II III IV

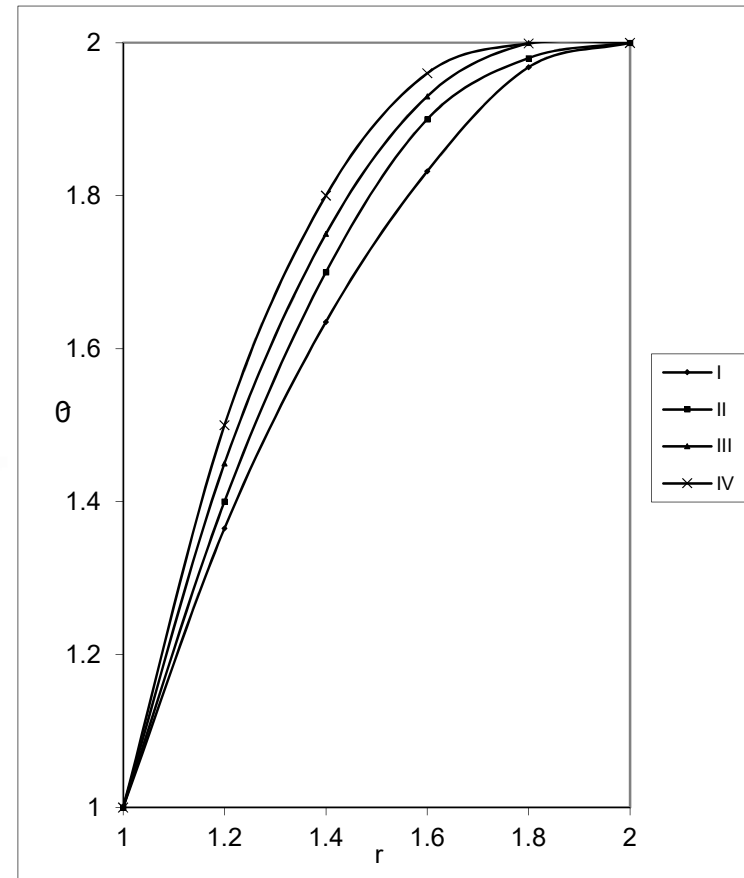


Fig.12  $\theta$  with Sc  
 I II III IV  
 Sc 0.24 0.6 1.3 2.01

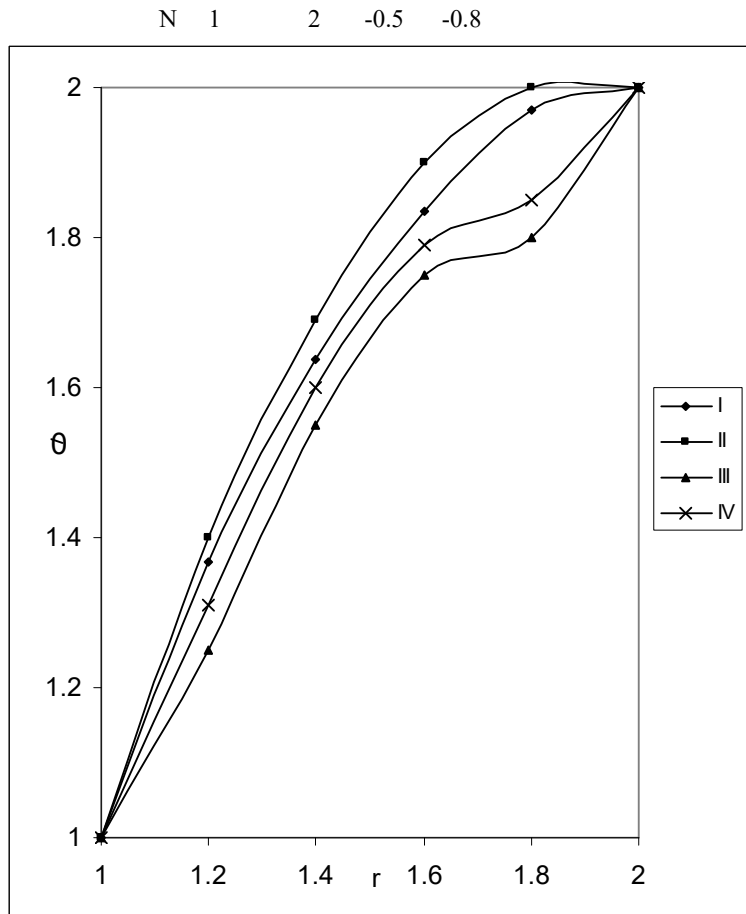


Fig.13  $\theta$  with  $S_0$   
 $Sc=1.3, n=1, m=2, \alpha=2$   
 I      II      III      IV

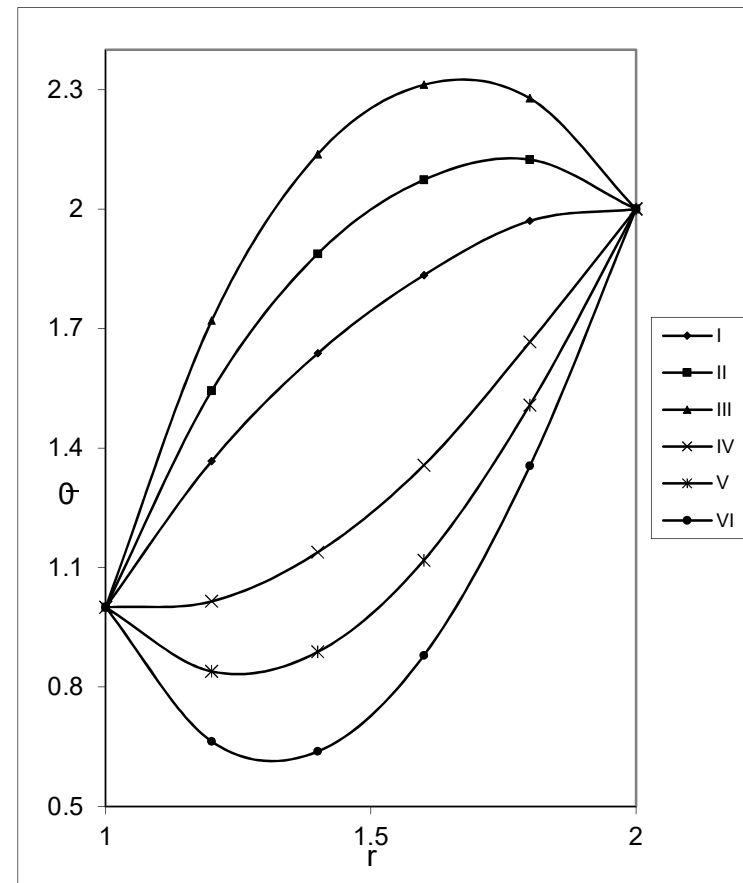


Fig.14  $\theta$  with  $\alpha$   
 $N=1, Sc=1.3, Sc=0.3, M=2$   
 I      II      III      IV      V      VI

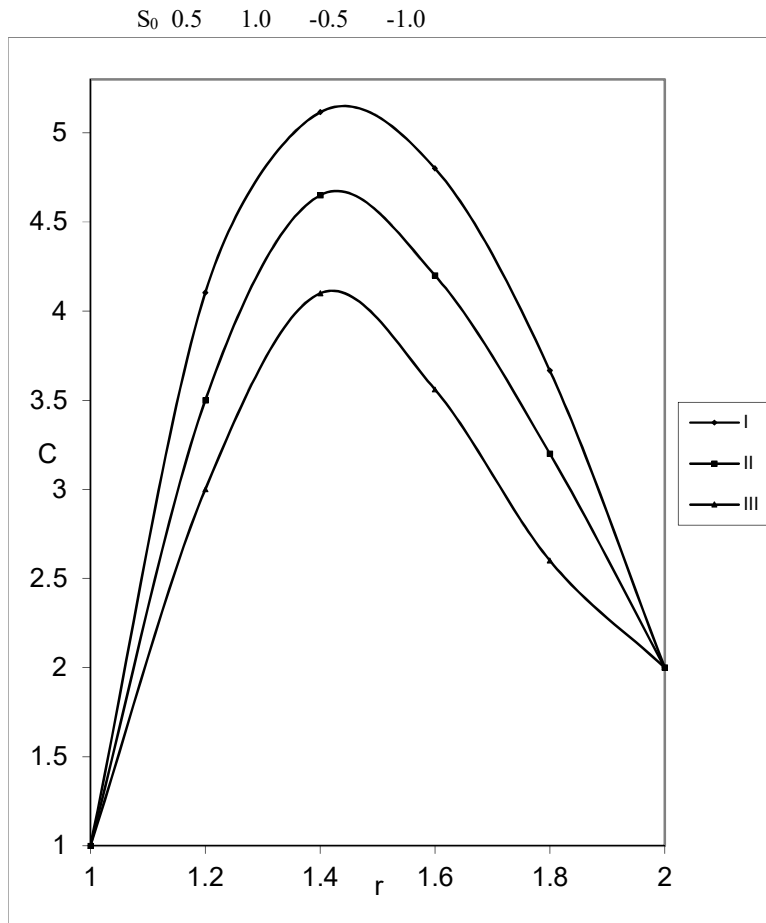


Fig.15 Variation of concentration (c) with G  

I	III	IV
$G = 10^3$	$3 \times 10^3$	$5 \times 10^3$

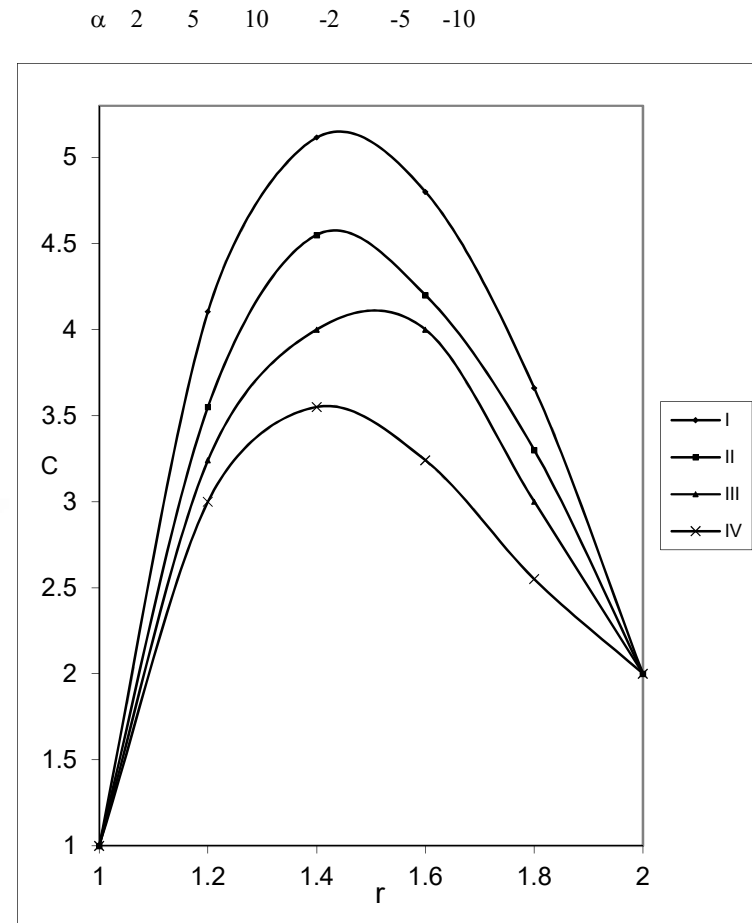


Fig.16 c with  $D^{-1}$   
 $G = 3 \times 10^3, M=2, \alpha=2$   

I	II	III	IV
---	----	-----	----

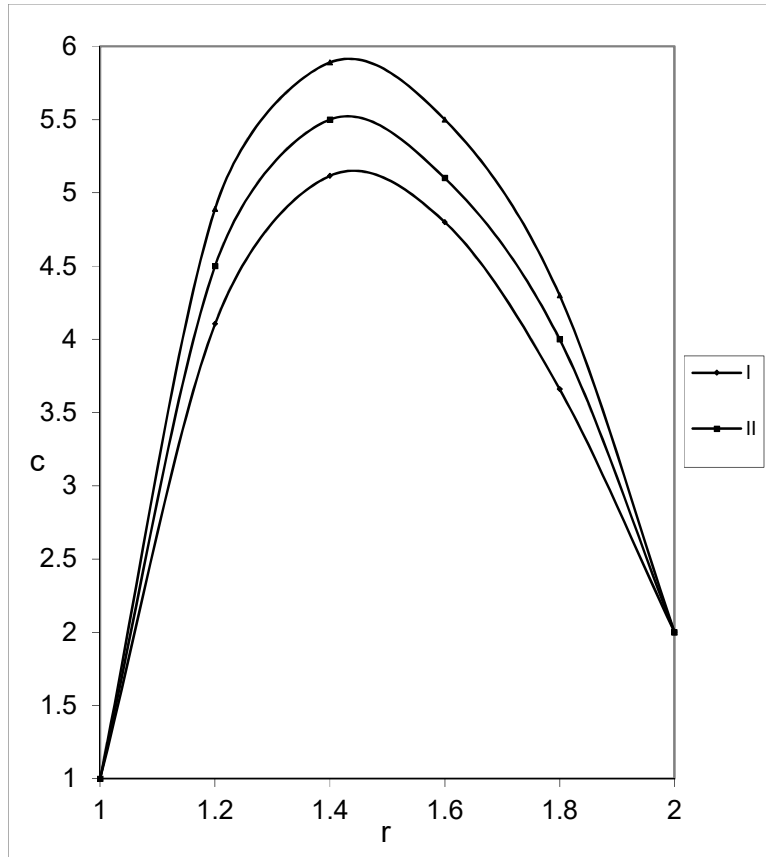


Fig.17 c with M  
 $G=3 \times 10^3, D^{-1}=10^3, \alpha=2$   

	I	II	III
M	2	3	5

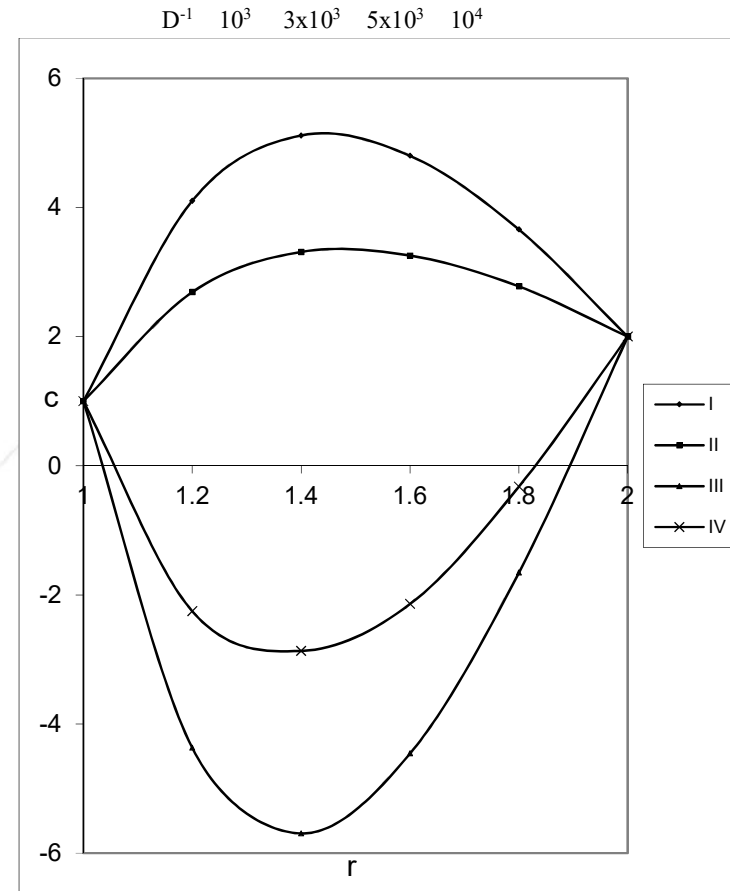


Fig.18 c with N  
 $G=3 \times 10^3, D^{-1}=10^3, M=2, \alpha=2$   

	I	II	III	IV
N	1	2	-0.5	-0.8

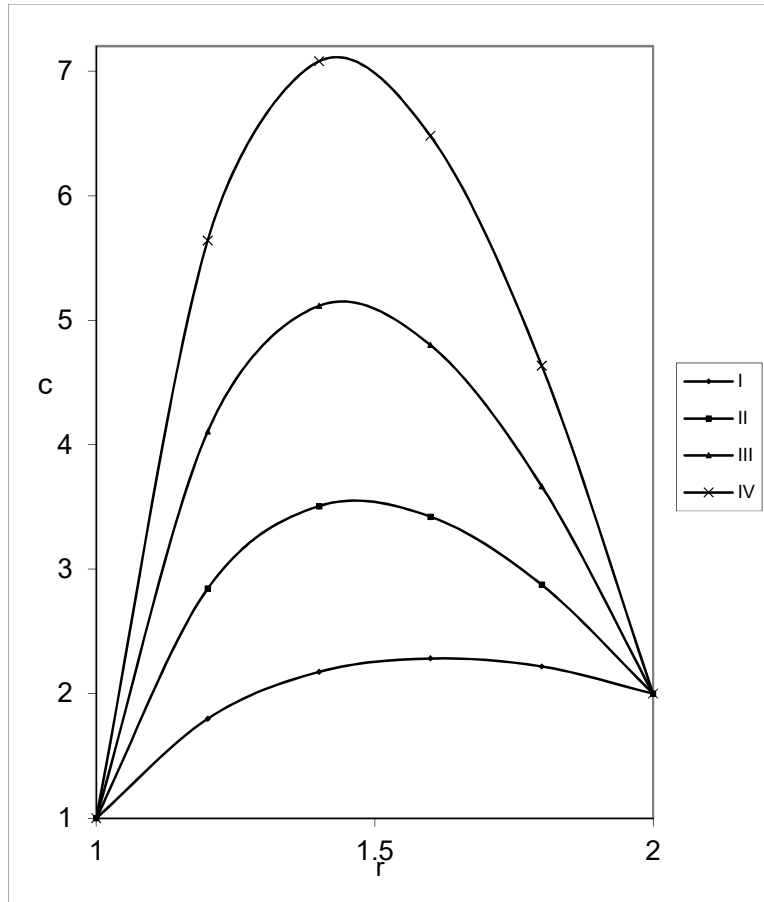


Fig.19  $\theta$  with  $Sc$   
I II III IV

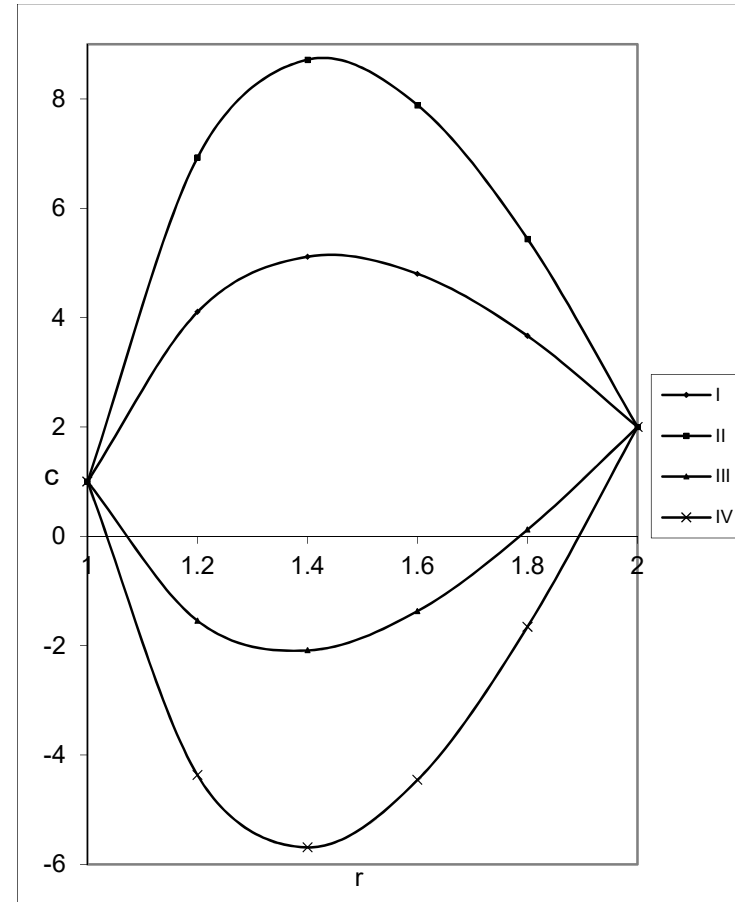


Fig.20  $\theta$  with  $S_0$   
 $Sc=1.3, N=1, M=2, \alpha=2$

Sc 0.24 0.6 1.3 2.01

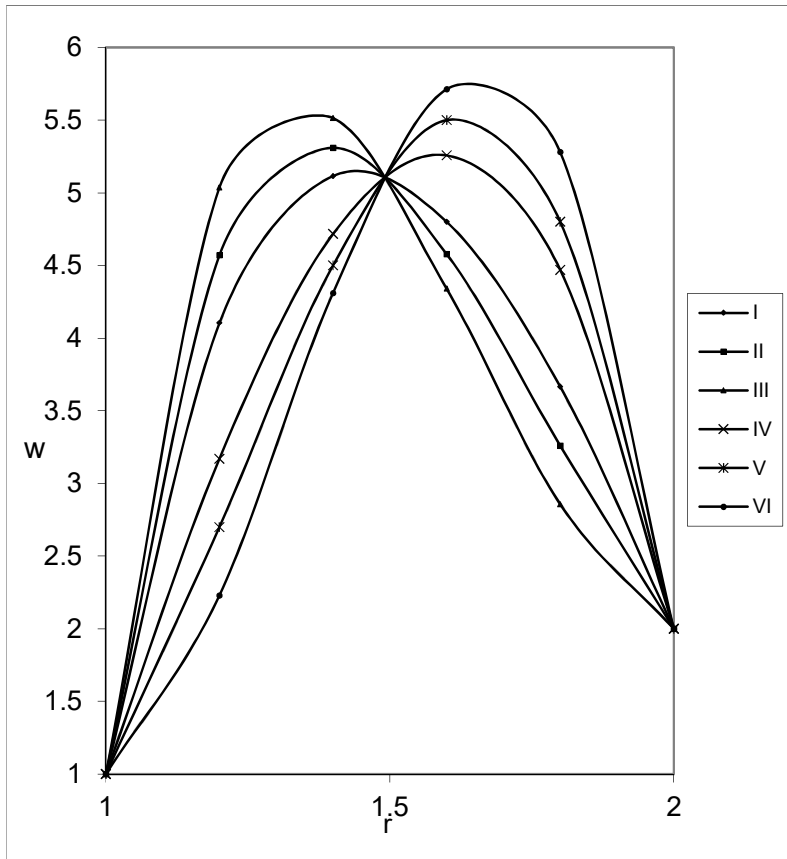


Fig.21  $w$  with  $\alpha$   
 $N=1, Sc=1.3, S_0=0.3, M=2$   
 I II III IV V VI

I II III IV  
 $S_0$  0.5 1.0 -0.5 -1.0

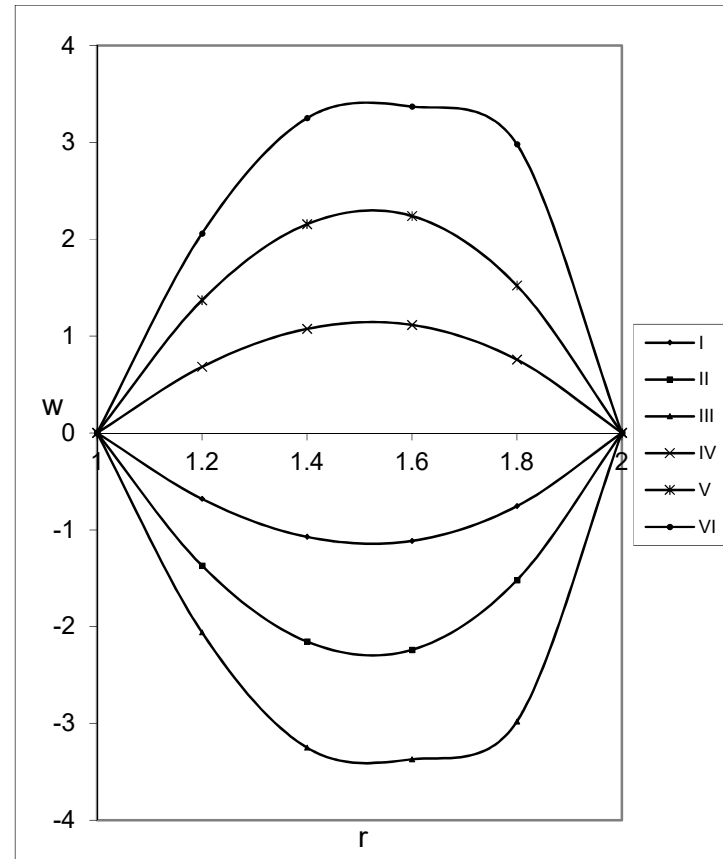


Fig.22 Variation of  $w$  with  $G$   
 $M=2, D^{-1}=2 \times 10^3, P=0.71$   
 I II III IV V VI

$\alpha$  2 5 10 -2 -5 -10

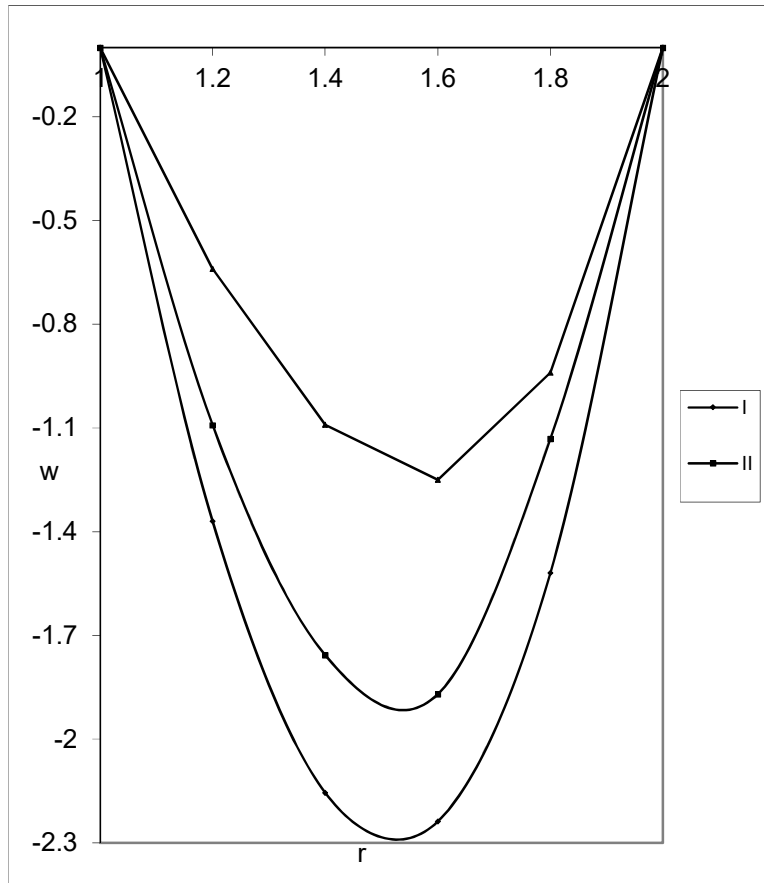


Fig.23 w with M  
 $G = 3 \times 10^3, D^{-1} = 10^3, \alpha = 2$

G  $10^3$   $3 \times 10^3$   $5 \times 10^3$   $-10^3$   $-3 \times 10^3$   $-5 \times 10^3$

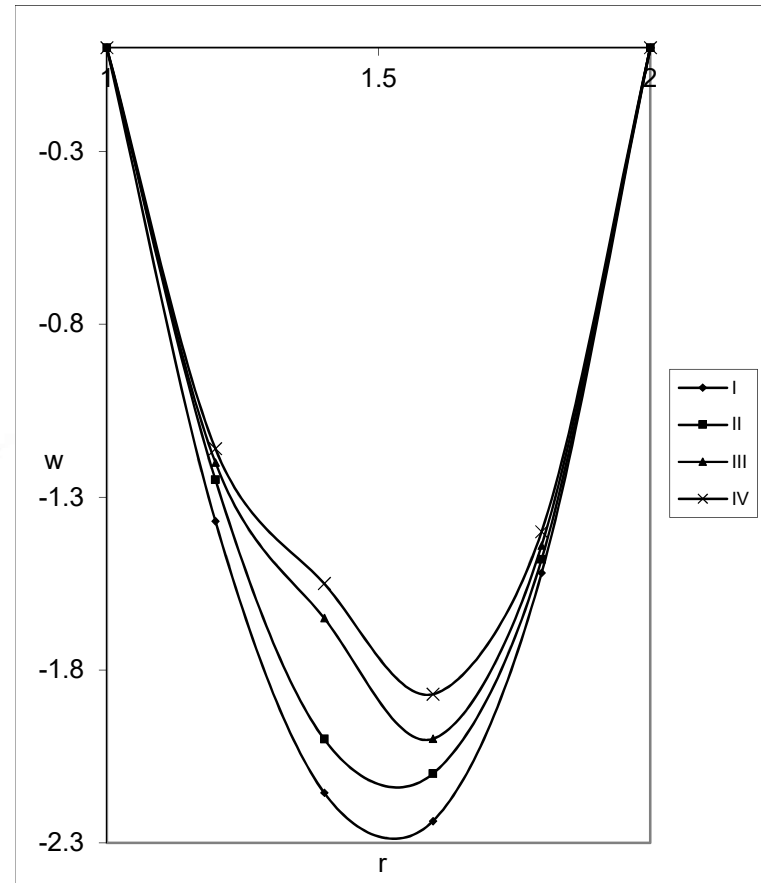


Fig.24 w with  $D^{-1}$   
 $\alpha = 2, M = 2, G = 3 \times 10^3$

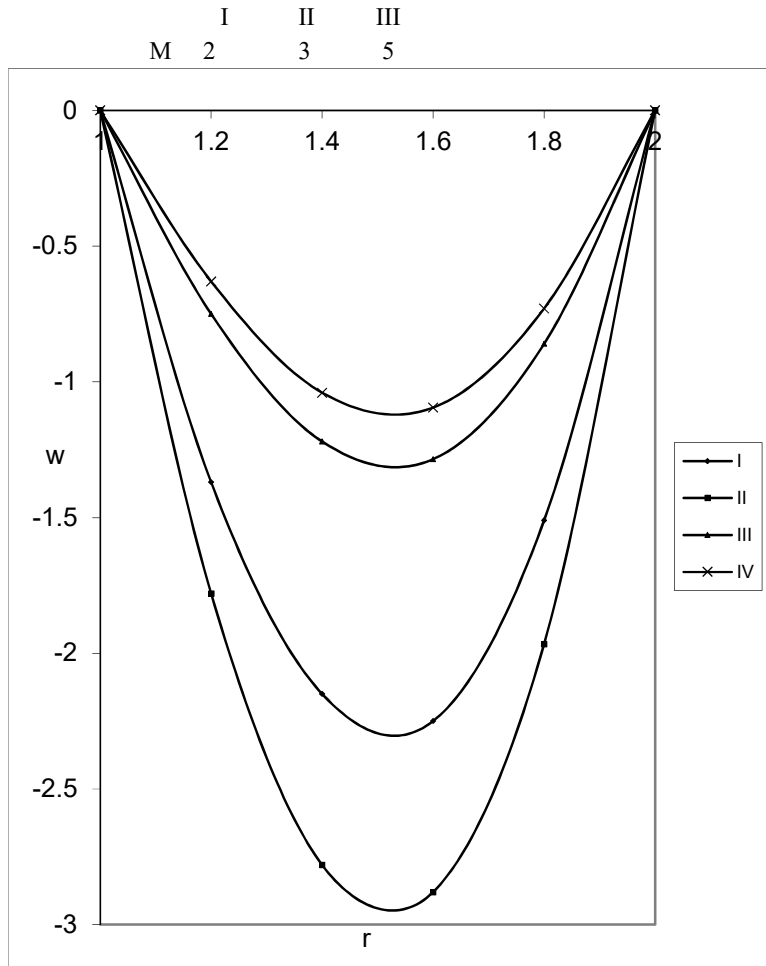


Fig.25 w with N

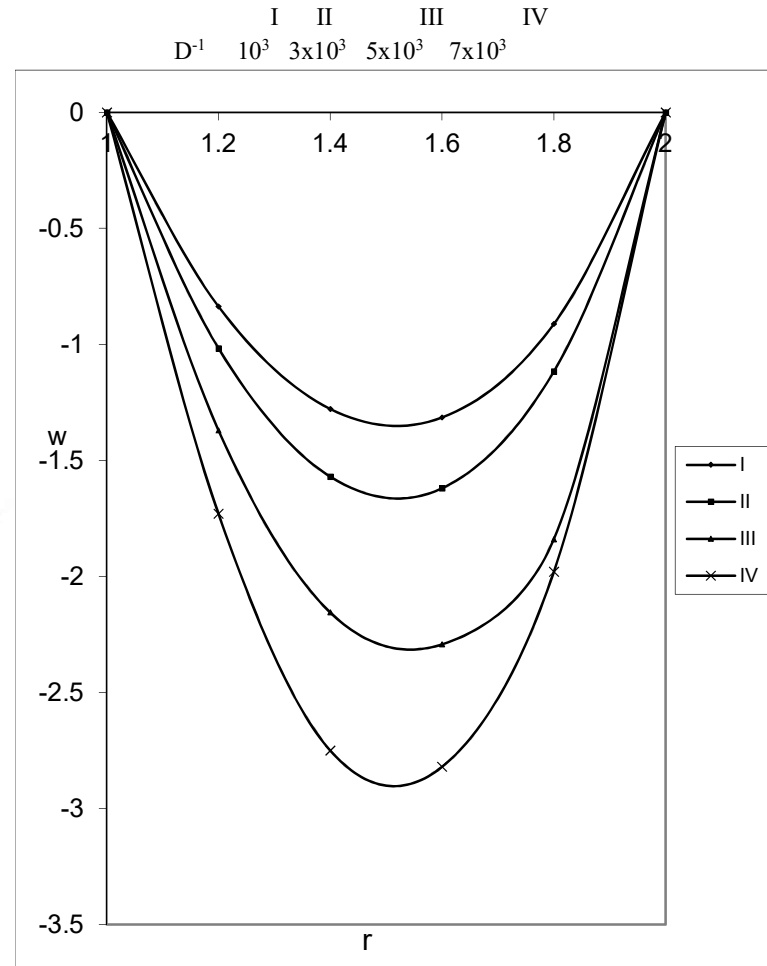


Fig.26 w with Sc

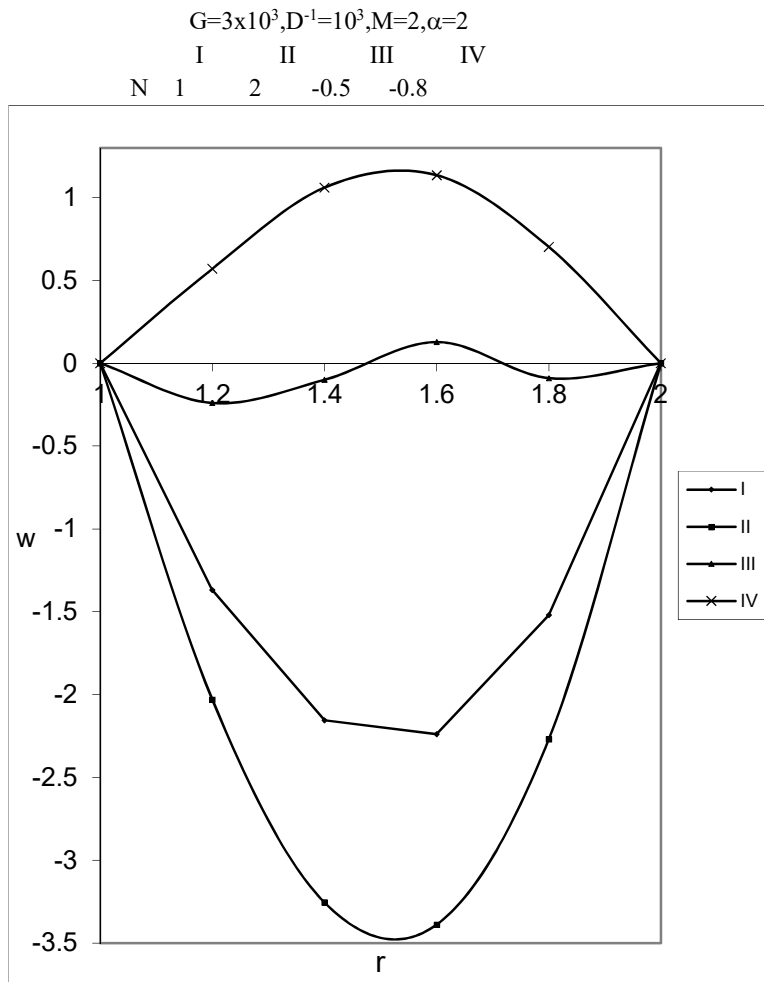


Fig.27 w with  $S_0$

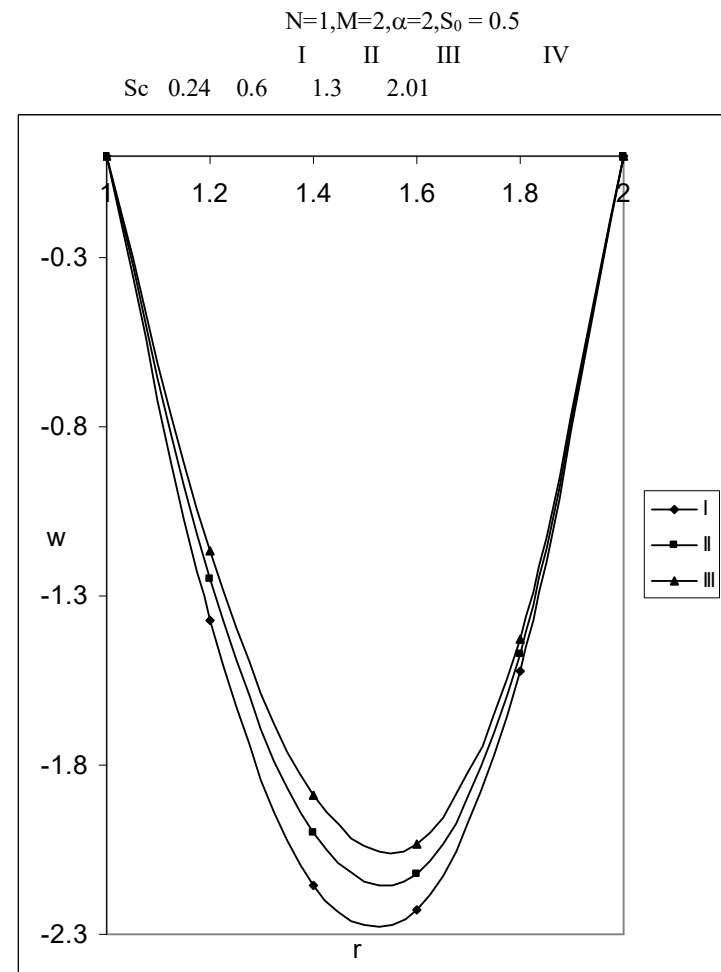
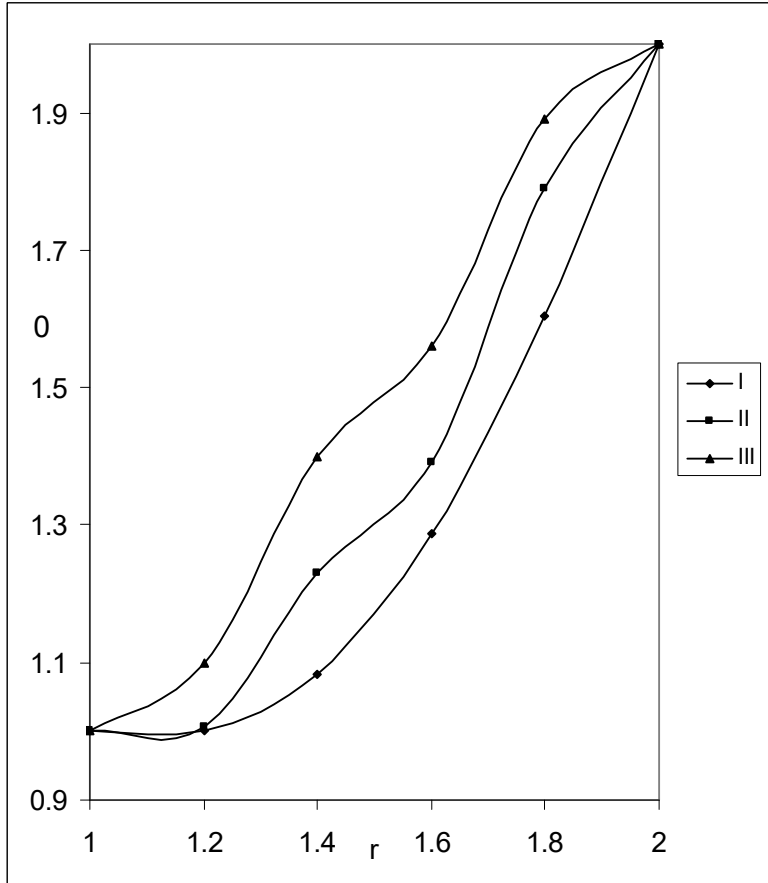


Fig.28 w with  $\alpha$

$Sc=1.3, N=1, M=2, D^{-1}=10^3$   
 I II III IV  
 $S_0$  0.5 1 -0.5 -1.0



$M=2, Sc=1.3, Sc=0.5, N=1$   
 I II III  
 $\alpha$  2 4 6

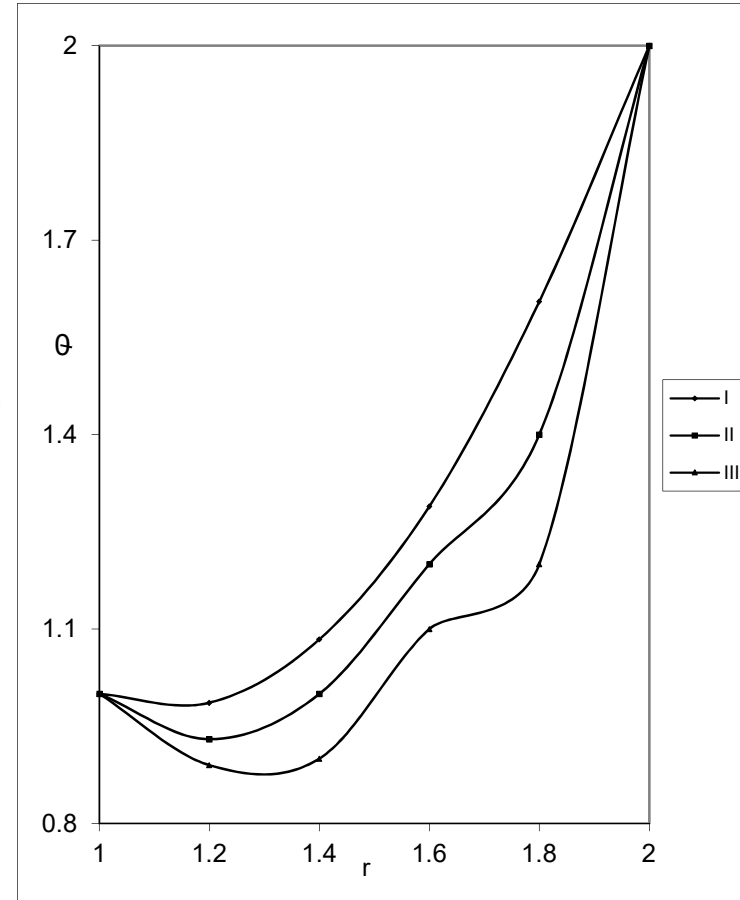


Fig.29 Variation of temperature( $\theta$ ) with G  
 $D^{-1}=10^3, N=1, Sc=1.3, M=2$   
 I II III  
 G  $10^3$   $3 \times 10^3$   $5 \times 10^3$

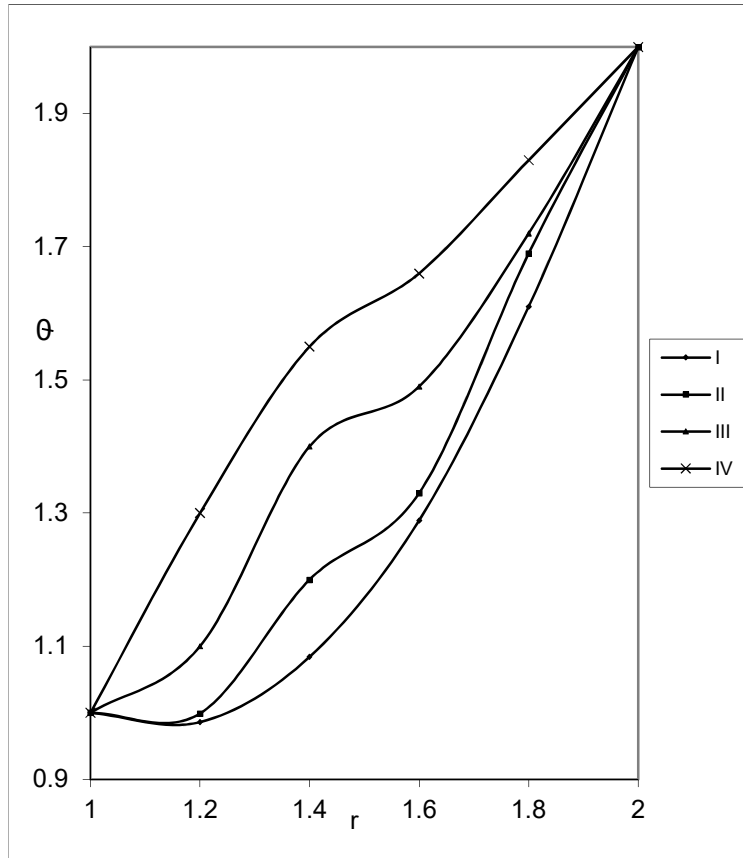


Fig.31  $\theta$  with  $D^{-1}$

Fig.30  $\theta$  with M  
 $D^{-1}=10^3, G=3 \times 10^3, N=1$   
 I II III  
 M 2 3 5

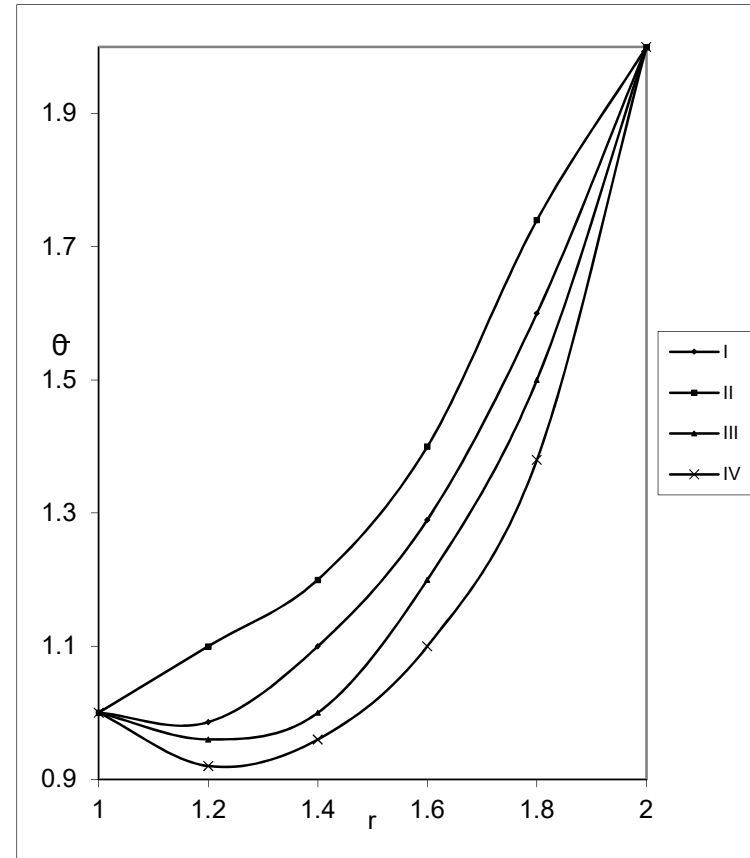


Fig.32  $\theta$  with N

	I	II	III	IV
$D^{-1}$	$10^3$	$3 \times 10^3$	$5 \times 10^3$	$7 \times 10^3$

	$M=2, Sc=1.3, S_0=0.5$			
	I	II	III	IV
N	1	2	-0.5	-0.8

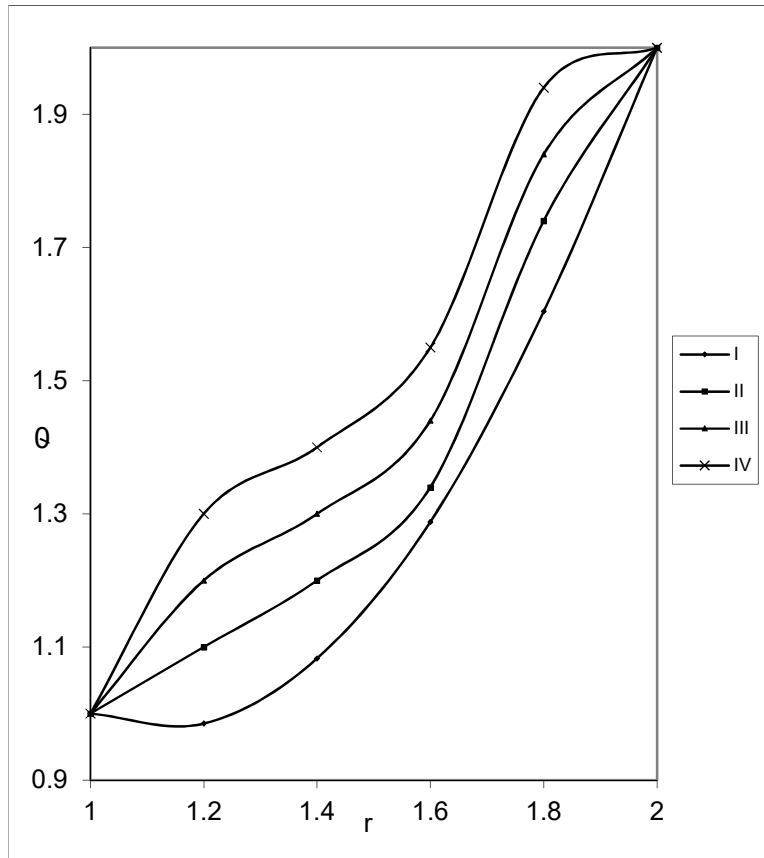


Fig.33  $\theta$  with Sc

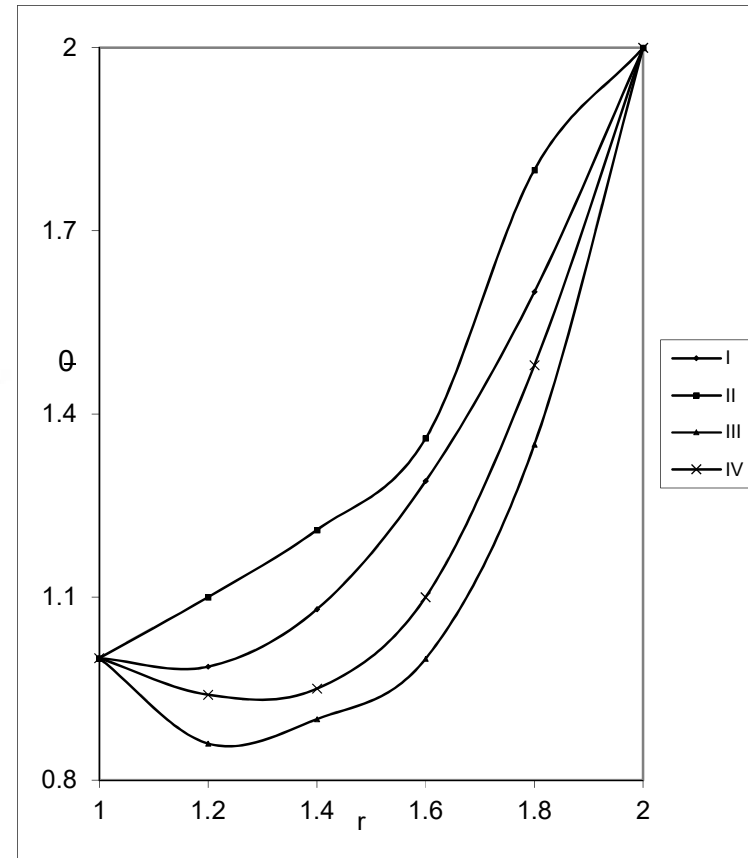
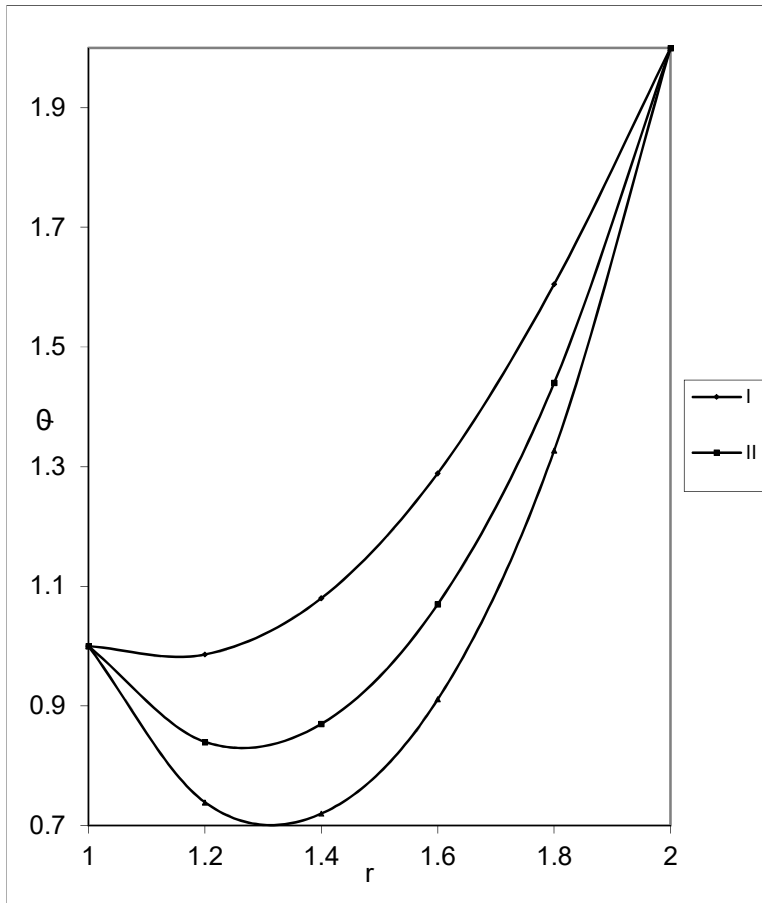


Fig.34  $\theta$  with  $S_0$

$S_0 = 0.5, N=1, M=2$   
 I II III IV  
 $Sc$  0.24 0.6 1.3 2.01



$Sc=1.3, N=1, M=2, \alpha=2$   
 I II III IV  
 $S_0$  0.5 1.0 -0.5 -1.0

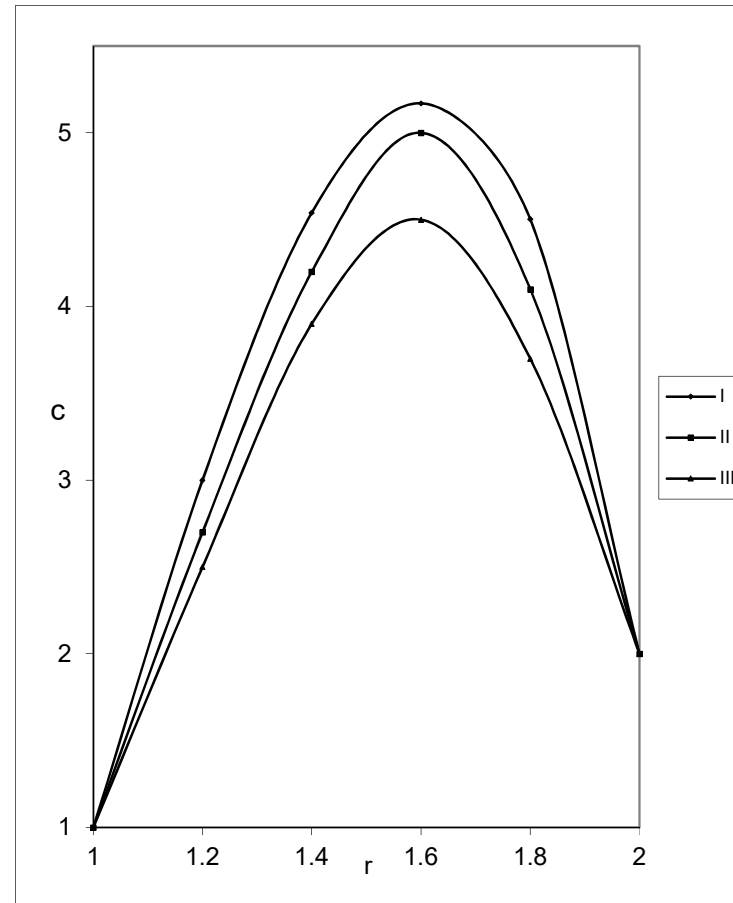




Fig.35  $\theta$  with  $\alpha$   
M=1,N=1,Sc=1.3,S<sub>0</sub>=0.5  
I II III  
 $\alpha$  2 4 6

Fig.36 Variation of concentration(c) with G  
D<sup>-1</sup>=10<sup>3</sup>,M=2,N=1, $\alpha$ =2  
I II III  
G 10<sup>3</sup> 3x10<sup>3</sup> 5x10<sup>3</sup>

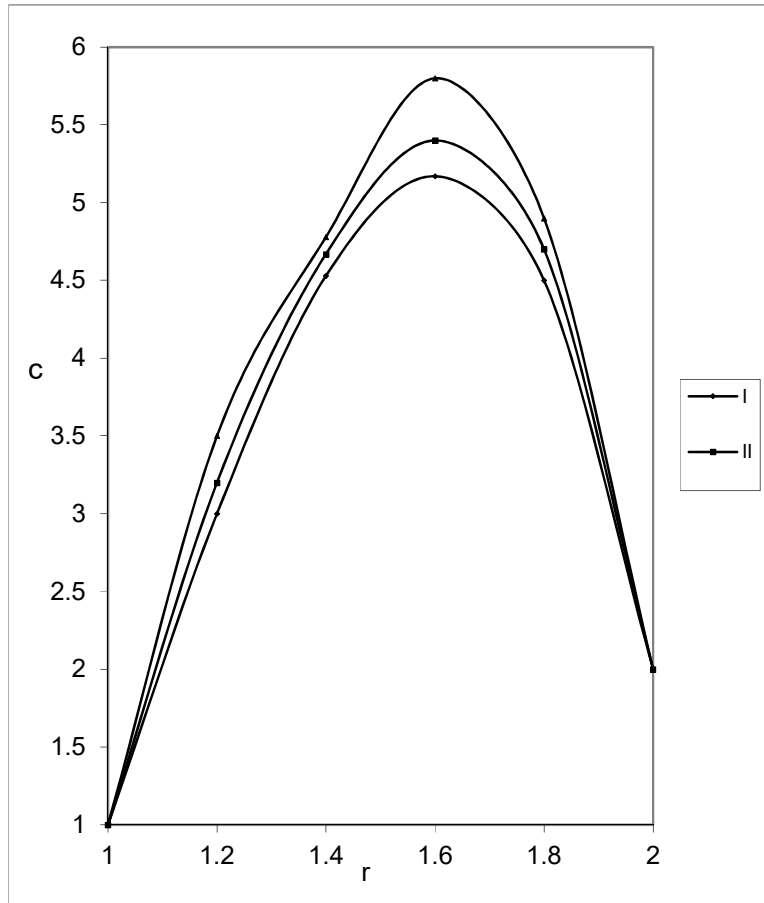


Fig.37 C with M  
 $D^{-1}=10^3, G=3 \times 10^3, M=2, N=1$   
 I II III

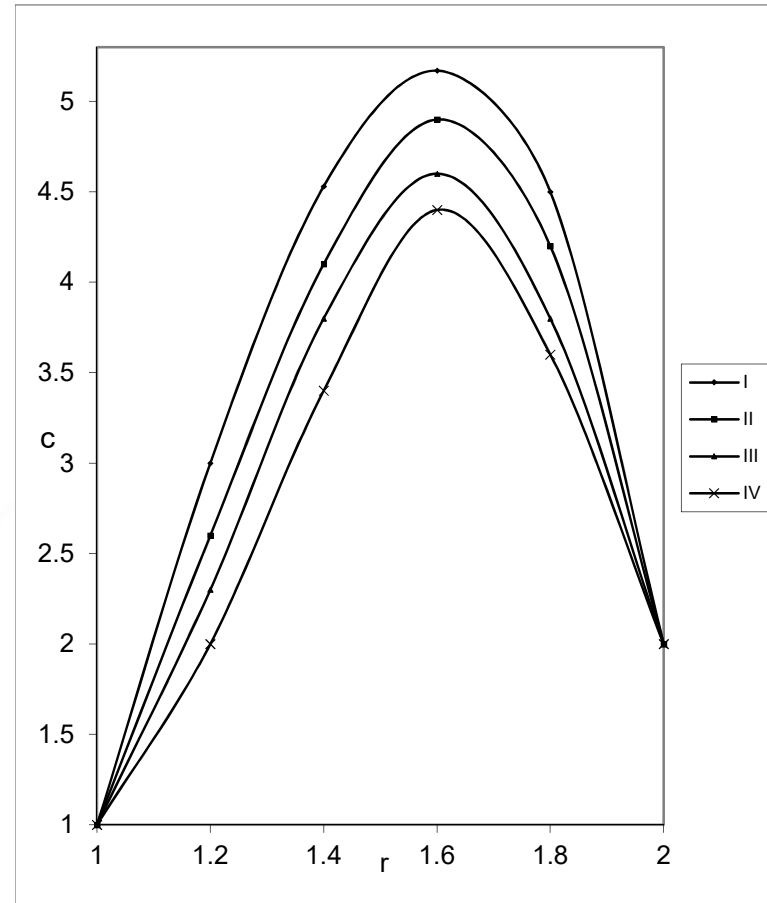


Fig.38 c with  $D^{-1}$   
 I II III IV  
 $D^{-1} \quad 10^3 \quad 3 \times 10^3 \quad 5 \times 10^3 \quad 7 \times 10^3$

M 23 5

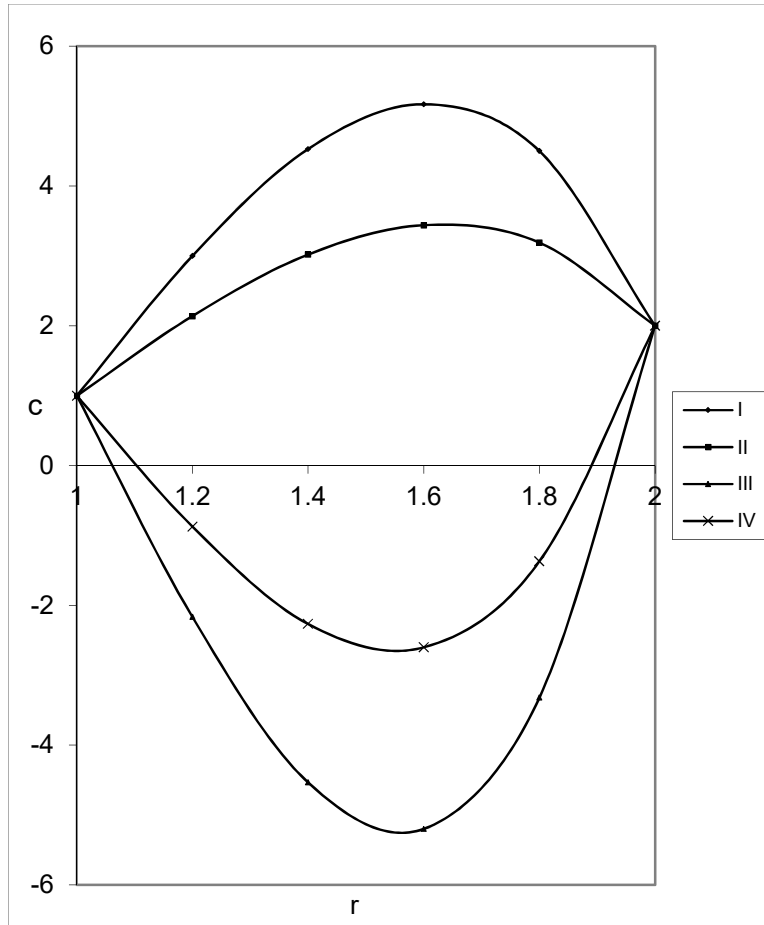


Fig.39 c with N  
I II III IV

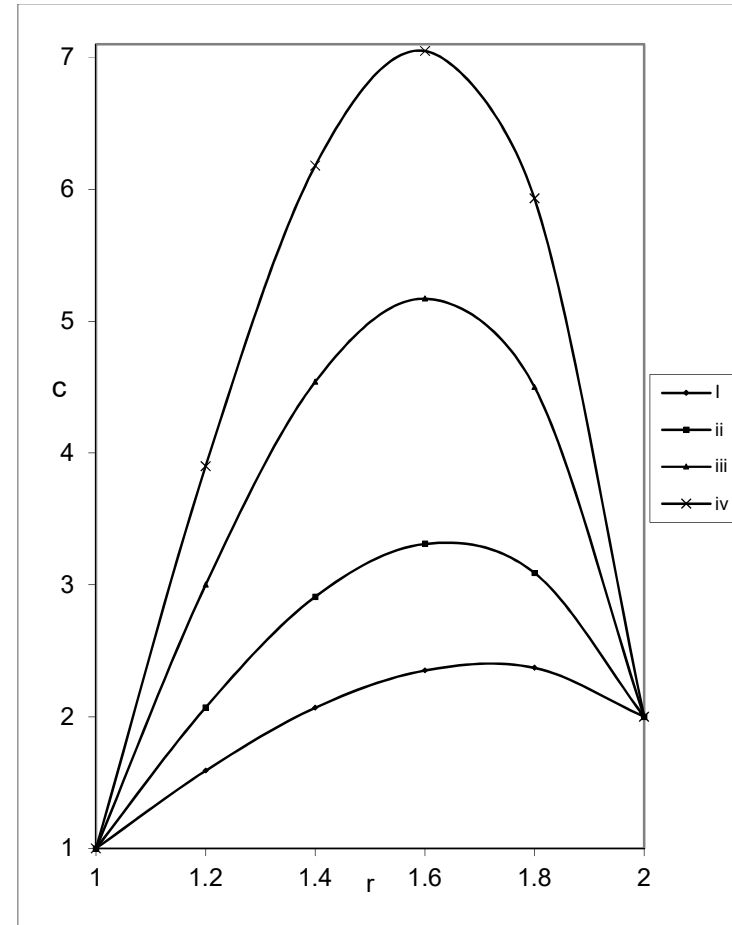


Fig.40 c with Sc  
I II III IV

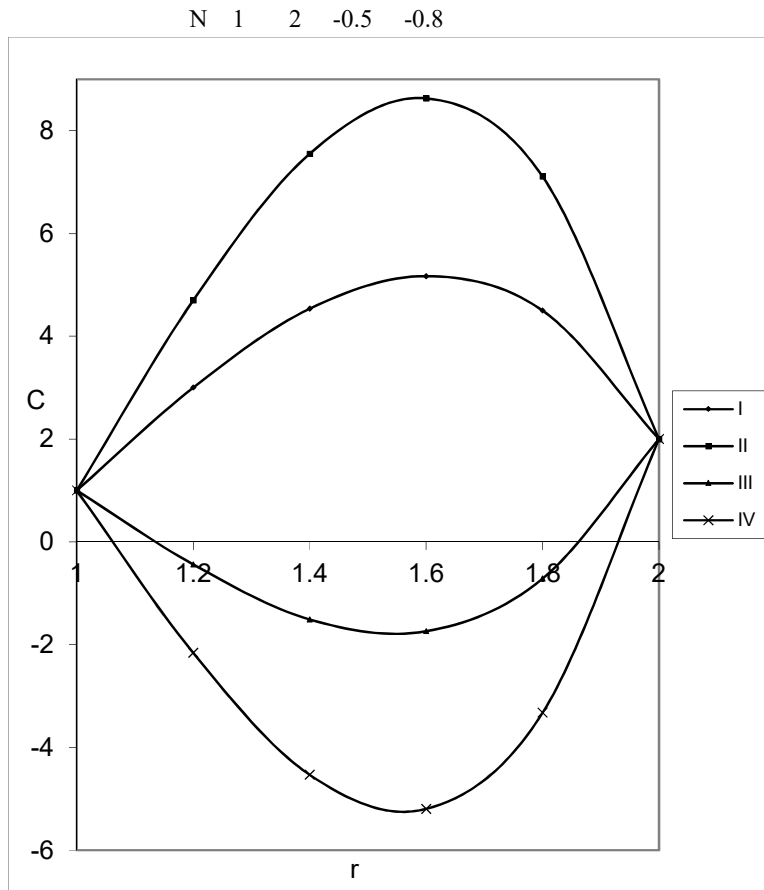


Fig.41  $c$  with  $S_0$   
 $Sc=1.3, N=1, M=2, \alpha=2$   
 I II III IV

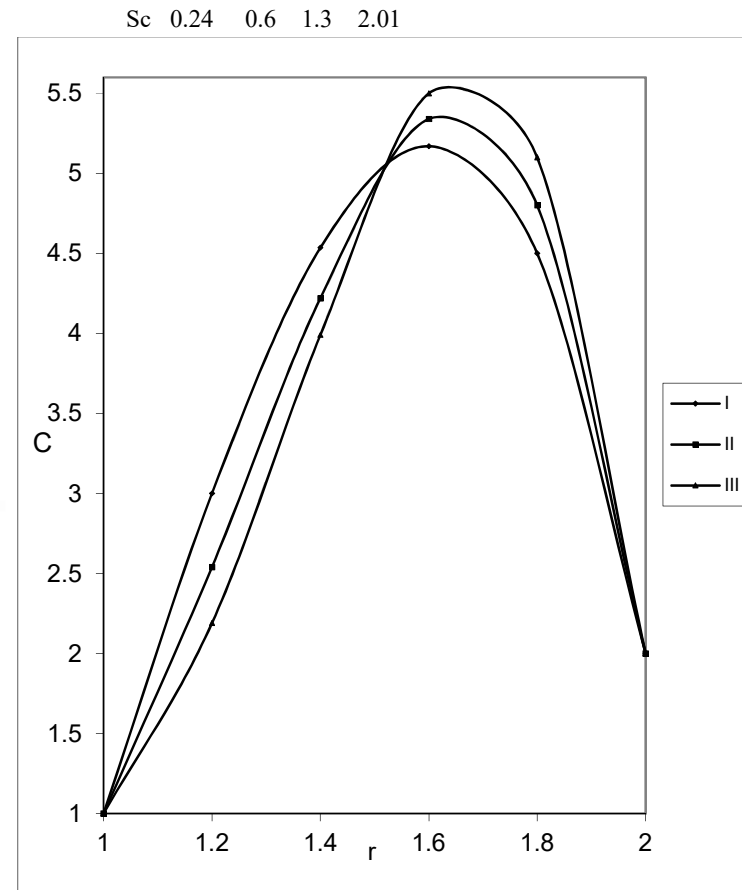


Fig.42  $c$  with  $\alpha$   
 $M=2, Sc=1.3, S_0=0.5, N=1$   
 I II III

Table.1  
Nusselt Number(Nu)  $r=1$   
 $P=0.71, N=1, Sc=1.3, S_0=0.5$

$G/\tau$	I	II	III	IV	V
$10^3$	-0.30746	-0.30891	-0.31061	-0.30171	-0.28920
$3 \times 10^3$	-0.28535	-0.29440	-0.30510	-0.24927	-0.22726
$5 \times 10^3$	-0.20629	-0.24254	-0.28539	1.53864	0.02633
$-10^3$	-0.30746	-0.30891	-0.31061	-0.30171	-0.28920
$-3 \times 10^3$	-0.28535	-0.29440	-0.30510	-0.24927	-0.22726
$-5 \times 10^3$	-0.20629	-0.24254	-0.28539	1.53864	0.02633

	I	II	III	IV	V
M	2	4	6	2	2
$D^{-1}$	$10^3$	$10^3$	$10^3$	$3 \times 10^3$	$5 \times 10^3$

Table.2  
Nusselt Number(Nu) at  $r=1$   
 $P=0.71, M=2, D^{-1}=10^3$

$G/\tau$	I	II	III
$10^3$	-0.30746	-1.20242	-1.88216
$3 \times 10^3$	-0.28535	-1.18507	-1.86804
$5 \times 10^3$	-0.20629	-1.12304	-1.81757
$-10^3$	-0.30746	-1.20242	-1.88216
$-3 \times 10^3$	-0.28535	-1.18507	-1.86804
$-5 \times 10^3$	-0.20629	-1.12304	-1.81757

	I	II	III
$\alpha$	2	4	6

Table.3  
Nusselt Number(Nu) at  $r=1$   
 $P=0.71, M=2, D^{-1}=10^3$

$G/\tau$	I	II	III	IV
$10^3$	-0.307612	-0.30467	-0.30877	-0.31070
$3 \times 10^3$	-0.28535	-0.26788	-0.30325	-0.30564

$5 \times 10^3$	-0.20629	-0.13637	-0.27798	-0.28753
$-10^3$	-0.307612	-0.30467	-0.30877	-0.31070
$-3 \times 10^3$	-0.28535	-0.26788	-0.30325	-0.30564
$-5 \times 10^3$	-0.20629	-0.13637	-0.27798	-0.28753
	I	II	III	IV
N	1	2	-0.5	-0.8

Table.4  
Nusselt Number(Nu) at  $r=1$   
 $P=0.71, M=2, D^{-1}=10^3$

$G/\tau$	I	II	III	IV
$10^3$	-0.23177	-0.27936	-0.30467	-0.30492
$3 \times 10^3$	-0.30213	-0.29738	-0.28535	-0.26940
$5 \times 10^3$	-0.27347	-0.25443	-0.20629	-0.14248
$-10^3$	-0.23177	-0.27936	-0.30467	-0.30492
$-3 \times 10^3$	-0.30213	-0.29738	-0.28535	-0.26940
$-5 \times 10^3$	-0.27347	-0.25443	-0.20629	-0.14248
	I	II	III	IV
Sc	0.24	0.6	1.3	2.01

Table.5  
Nusselt Number(Nu) at  $r=1$   
 $P=0.71, M=2, D^{-1}=10^3$

$G/\tau$	I	II	III	IV
$10^3$	-0.30746	-0.30234	-0.31151	-0.31071
$3 \times 10^3$	-0.28535	-0.25328	-0.31146	-0.30568
$5 \times 10^3$	-0.20629	-0.07794	-0.31105	-0.28770
$-10^3$	-0.30746	-0.30234	-0.31151	-0.31071
$-3 \times 10^3$	-0.28535	-0.25328	-0.31146	-0.30568

$-5 \times 10^3$	-0.20629	-0.07794	-0.31105	-0.28770
------------------	----------	----------	----------	----------

	I	II	III	IV
$S_0$	0.5	1.0	-0.5	-1.0

Table.6  
Nusselt Number(Nu) at the outer cylinder  $r=2$   
 $P=0.71, N=1, Sc=1.3, S_0=0.5$

$G/\tau$	I	II	III	IV	V
$10^3$	1.53394	1.53495	1.53629	1.52910	1.52612
$3 \times 10^3$	1.51543	1.52177	1.53014	1.48504	1.46638
$5 \times 10^3$	1.44927	1.47464	1.50817	0.58744	1.25288
$-10^3$	1.53394	1.53495	1.53629	1.52910	1.52612
$-3 \times 10^3$	1.51543	1.52177	1.53014	1.48504	1.46638
$-5 \times 10^3$	1.44927	1.47464	1.50817	0.58744	1.25288

	I	II	III	IV	V
M	2	4	6	2	2
$D^{-1}$	$10^3$	$10^3$	$10^3$	$3 \times 10^3$	$5 \times 10^3$

Table.7  
Nusselt Number(Nu) at  $r=2$   
 $P=0.71, M=2, D^{-1}=10^3$

$G/\tau$	I	II	III
$10^3$	1.53394	2.57222	3.42277
$3 \times 10^3$	1.51543	2.55665	3.40928
$5 \times 10^3$	1.44927	2.50100	3.36108
$-10^3$	1.53394	2.57222	3.42277
$-3 \times 10^3$	1.51543	2.55665	3.40928
$-5 \times 10^3$	1.44927	2.50100	3.36108

	I	II	III
$\alpha$	2	4	6

Table.8

 Nusselt Number(Nu) at  $r=2$ 
 $P=0.71, M=2, D^{-1}=10^3$ 

$G/\tau$	I	II	III	IV
$10^3$	1.53394	1.53170	1.55012	1.53660
$3 \times 10^3$	1.51543	1.50137	1.53006	1.53205
$5 \times 10^3$	1.44927	1.39300	1.50780	1.51578
$-10^3$	1.53394	1.53170	1.55012	1.53660
$-3 \times 10^3$	1.51543	1.50137	1.53006	1.53205
$-5 \times 10^3$	1.44927	1.39300	1.50780	1.51578

	I	II	III	IV
N	1	2	-0.5	-0.8

Table.9

 Nusselt Number(Nu) at  $r=2$ 
 $P=0.71, M=2, D^{-1}=10^3$ 

$G/\tau$	I	II	III	IV
$10^3$	1.19513	1.50919	1.53394	1.53173
$3 \times 10^3$	1.52987	1.52581	1.51543	1.50155
$5 \times 10^3$	1.50704	1.49080	1.44927	1.39371
$-10^3$	1.19513	1.50919	1.53394	1.53173
$-3 \times 10^3$	1.52987	1.52581	1.51543	1.50155
$-5 \times 10^3$	1.50704	1.49080	1.44927	1.39371

	I	II	III	IV
Sc	0.24	0.6	1.3	2.01

Table.10

 Nusselt Number(Nu) at  $r=2$ 
 $P=0.71, M=2, D^{-1}=10^3$ 

$G/\tau$	I	II	III	IV
----------	---	----	-----	----

$10^3$	1.53394	1.52947	1.53737	1.53650
$3 \times 10^3$	1.51543	1.48744	1.53637	1.53146
$5 \times 10^3$	1.44927	1.33724	1.53627	1.51343
$-10^3$	1.53394	1.52947	1.53737	1.53650
$-3 \times 10^3$	1.51543	1.48744	1.53637	1.53146
$-5 \times 10^3$	1.44927	1.33724	1.53627	1.51343

	I	II	III	IV
$S_0$	0.5	1.0	-0.5	-1.0

## 6. References

- Costa, V.A.F.: Thermodynamics of natural convection in enclosures with viscous dissipation, *Int. Jour. Heat Mass Transfer*, V.48, pp.2333-2341(2005).
- Dephew, C.A, and August. S.E : *Trans. Ame. Soc. Mech. Engng ser C*, J. Heat Transfer, V.93, P.350 (1971).
- Deshikarchar, K.S and Ramachandra Rao, A, *Physics fluids* V.30, P.278 (1987).
- Faghri, M. and Welty, J.R. V.21, P.317 (1978)
- Gill, W.M. and Casal, A.D., *Ame. Chemical Engineering journal* V.B.P 570 (1962).
- Heinbochal, J.H and Ash, R.L., *ZAMP*, V.21.P.266 (1970).
- Krishna D.V. Kalposchikov, V.L, Martynenko, O.G, Shabunya, S.I., Shnip, A.I, Luikov, A.V, "Reports from Lukov Heat and Mass Transport Institute of Minsk, U.S.S.R(1985)
- Krishna D.V, Prasada Rao, D.R.V and Sarojamma.G : *Int. Comm.Heat and Mass Transfer*, V.16, P.237(1988.)
- Morton, B.R, Q.J. *Mechanical, Application . Maths*, V.12, P.410 (1959).
- Morton, B.R, *J.Fluid. Mech.*, V.8, P.27(1960).
- Mc Michael, M and Deutsch, S. "Physics fluids", V.27(1), P.110 (1984).
- Reynolds, W.C., *Trans. Ame. Soc. Mech. Engg. Ser*, V. C.J. Heat transfer, v.82, P.108 (1960).
- Simpkins, P.G, Greenberg-Kosinski, S. an Macchesney, J.B., *J.Appl. Physics* .V.50(9), P.5676(1979).
- Simpkins, P.G, Greenberg-Kosinski, S., and Maaechaney, J.B, *J.Appl. Physics*, V.50(a), P.238, (1979).
- Sree Ramanchandra Murthy, A., Buoyancy induced hydromagnetic flows through a porous medium –A study, Ph.D thesis submitted to S.K.University, Anantapur, India (1992)
- Tanmay Basak, S.Roy, T.Paul, I.Pop.: Natural convection in a square cavity filled with a porous medium : Effects of various thermal boundary conditions., *Int.J. Heat and Mass transfer*, V.49, pp.1430-1441(2006) .
- Waller, K.L., George, M., Magry and Franz.t, Geyling, *J.colloid Interface Science*, V.69(1), P.138(1979).
- Wlaker, K.L., Geyling . F.T and Nagel, S.R .J *Ame. Ceram. Science*, V.63 (9), P.552(1980).